MCnebula: Critical chemical classes to classify and boost identification by visualization for untargeted LC-MS/MS data analysis

Lichuang Huang[1, 2 #], Qiyuan Shan[1, 2 #], Qiang Lyu[1], Shuosheng Zhang[3], Lu Wang[1, 2*], Gang Cao[1, 2*]

[1] School of Pharmacy, Zhejiang Chinese Medical University, Hangzhou, China

[2] Jinhua Institute, Zhejiang Chinese Medical University, Hangzhou, China

[3] College of Chinese Materia Medica and Food Engineering, Shanxi University of Chinese Medicine, Jinzhong, China.

[#]These authors contributed equally to this work

*Address correspondence to:

Lu Wang, Ph.D.

School of Pharmacy, Zhejiang Chinese Medical University, No. 548 Binwen Road, Hangzhou, Zhejiang 310053, China; E-mail: luwang0520@163.com

Professor Gang Cao, Ph.D.

School of Pharmacy, Zhejiang Chinese Medical University, No. 548 Binwen Road, Hangzhou, Zhejiang 310053, China; Tel/Fax: +86 571 87195895; E-mail: caogang33@163.com

Abstract

Untargeted mass spectrometry is a robust tool for biology, but it usually requires much time on data analysis especially for system biology. We established a framework called MCnebula (Multiple-Chemical nebula) to facilitate mass spectrometry data analysis process by focusing on critical chemical classes and visualization in multiple dimensions. It consisted of three vital steps: (1) abundance-based classes (ABC) selection algorithm, (2) critical chemical classes to classify 'features' (compounds), (3) visualization as multiple Child-Nebulae (network graph) with annotation, chemical classification and structure. Notably, MCnebula can be applied to explore classification and structural characteristic of unknown compounds that beyond the limit of spectral library. What's more, it is intuitive and convenient for pathway analysis and biomarker discovery due to its function of ABC selection and visualization. MCnebula was implemented in the R language. We provided a series of tools in the R packages to facilitate downstream analysis in a MCnebula-featured way, including feature selection (statistical analysis of binary comparisons), homology tracing of top features, pathway enrichment analysis, heat map clustering analysis, spectral visualization analysis, chemical information query and output analysis reports, etc. In order to illustrate the broad utility of MCnebula, we investigated a human-derived serum dataset for metabolomics analysis. The results indicated that 'Acyl carnitines' were screened out by tracing structural classes of biomarkers which was consistent with the reference. We also investigated a plant-derived dataset of herbal *E. ulmoides* to achieve a rapid unknown compound annotation and discovery.

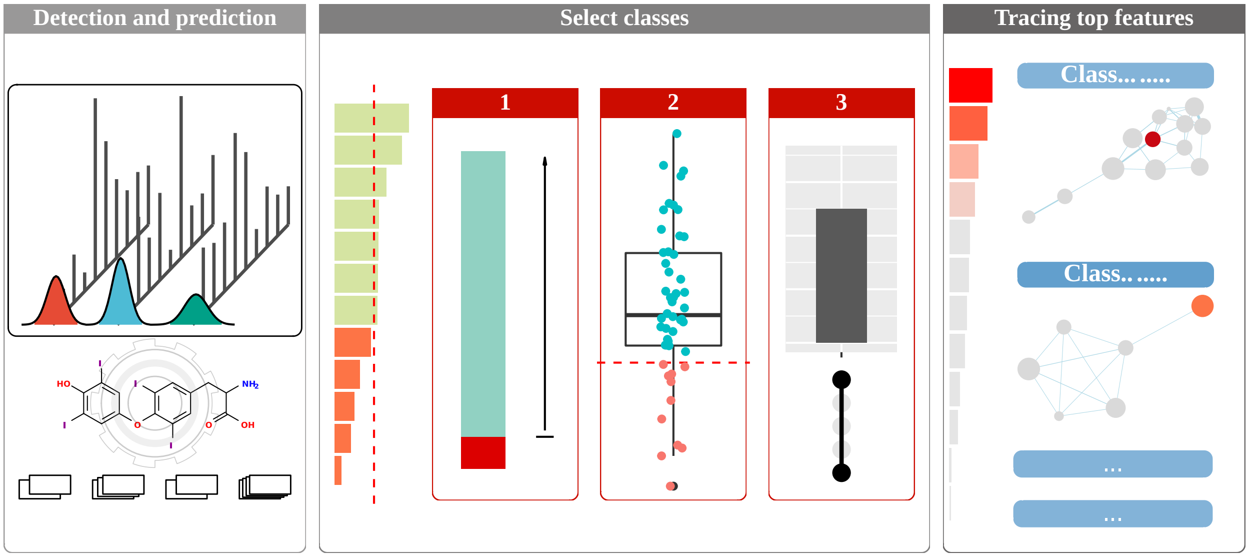

Keywords: Mass spectrometry, visualization, chemical classes, identification, MCnebula

Introduction

Analyzing untargeted liquid chromatography/tandem mass spectrometry (LC-MS/MS) dataset is complicated, due to the massive of data volume, complexity of spectra and structural diversity of compounds. In the past decades, a lot of researchers attempted to address the issues. Many technical software or web-based interfaces were developed to provide a one-stop bulk solution for data analysis[1–4]. These solutions applied or suggested flexible mass spectra processing tools or analogous algorithms[5–8]. To reduce false-positive and false-negative results, more algorithms have been implemented for peak deconvolution, feature selection or statistical filtering[9–12]. Every feature corresponding to a compound within sample or parallel samples was prevalently equipped with fragmentation spectra for identification. In this context, researchers have to be confronted with a problem: how to identify so many compounds accurately and quickly?

Until today, several strategies were developed for identifying compounds with fragmentation spectra. **1)** Spectral library matching. A number of public available databases were built to settle that via achieving reusability of reference fragmentation spectra, such as MassBank, MassBank of North America (MoNA), Global Natural Products Society molecular networking (GNPS)[4]. In the meanwhile, these fragmentation spectra are available via their web servers, third-party platform (e.g., CompMass) or specific tools (MASST)[13]. However, compared with structure database (PubChem harbours over 100 million records), spectral library is too small in size that limit the application of mass spectrometry. To cross this barrier, **2)** *In silico* simulation by fragmentation spectra. *In silico* tools have been increasingly developed for simulating fragmentation spectra[14–17]. Some databases such as MoNA collated *in silico* fragmentation spectra and were available for public[18]. **3)** *In silico* prediction with matching learning. At present, the algorithms made machine training from reference mass dataset or libraries, then 'learned' how to predict chemical fingerprints or principles so as to retrieve the correct structure from structure database[19–21].

In silico methods are developing quickly. Up to now, the cutting-edge technology, called SIRIUS 4[22], integrated with many advanced algorithms of artificial intelligence, was reported that its accuracy rate reached to 70% while retrieving in structure libraries. This method helps to identify metabolites beyond the scope of spectral libraries. While *in silico* tools boost chemical identification, it is still lack of a proper framework that could incorporate and leverage SIRIUS 4 into user-friendly way for biological research, such as biomarker discovery and pathway analysis of mass spectral dataset. Compounds annotation and screening of biomarkers manually are both time-consuming and the results are impressed by subjective factors. Molecular networking is more and more popular due to its visualization and data transparency. Molecular networking was a spectral correlation and visualization method that can detect spectra from related molecules (so-called spectral networks), even when the spectra were not matched to any known compounds[4]. Based on the concept of molecular networking, we proposed an idea, clustering features for visualization of chemical classification probably contribute to the discovery of biomarkers and metabolic pathway analysis.

The history of classification in chemistry dated back to the middle of the last century. The Chemical Fragmentation Coding system was firstly developed by Derwent World Patent Index (DWPI) in 1963. Until recent years chemical classification like Gene Ontology (GO)[23] which was organized with taxonomy and ontology was proposed more systematically[24]. ClassyFire is popular for compound annotation in LC-MS dataset analysis due to its computation available and systematicness[25–28]. The taxonomy and ontology is robust and useful for chemistry. For example, a hierarchical classification-based method, called Qemistree, was proposed to analyze mass spectrometry data by expressing molecular relationships as a tree, which could be represented in the context of sample metadata and chemical ontologies[29].

Untargeted metabolomics is a field of omics science that uses cutting-edge analytical chemistry techniques and advanced computational methods to characterize complex biochemical mixtures aimlessly. LCMS-based untargeted metabolomics is very popular due to its high sensitivity, small sample volume and direct injection without separation etc.[30]. With the help of statistical methodologies, researchers could screen and identify more-informative disease biomarkers from thousands of LC-MS features, to aid the design or development of improved treatments and to better assess health outcomes[31]. . These statistical approaches mainly involved classical statistic and artificial intelligence models(e.g., random forests)[32]. Both approaches were inevitable to introduce specific biases, owing to the complexity of feature set or algorithmic stability[33]. Furthermore, analyzing at feature level was unable to profile systematic effects on metabolites unbiased[34]. In this view, analyzing at chemical classified level may be a better settlement. However, it shouldn't be ignored that the differences of metabolites at the same classified level. For example, small-molecules belonging to 'Indoles and derivatives' had structural dependent affection on aryl hydrocarbon receptor (AHR)[35]. Different structural characteristics will lead to diverse activities. The settlement for that is integrating both 'feature' level statistic and classified level assessment.

In addition to chemical classifying and statistical analysis, clustering visualization was also a popular tool for untargeted mass spectrometry data analysis. Over the last decade, Global Natural Products Social Molecular Networking (GNPS) is more and more popular as a clustering visualization tool based on MS dataset. GNPS applied molecular networking connecting mass spectra of molecules based on the similarity of their fragmentation patterns[36]. Unfortunately, molecular networking of GNPS mainly depend on on spectral similarity instead of compounds structural or classified similarity. For example, flavonoids consist of an aromatic ring joined to an oxygenated heterocyclic ring linked to a phenyl group,which were expected to be clustered together since its specific class and structural similarity. However, , it was reported that some compounds belonging to flavonoids happened to be absent from the cluster of other flavonoids compounds in previous research[34]. Thus, clustering visualization in a classified level is a better choice for untargeted mass spectra dataset. Earlier in 2012, the concept of molecular networking with visualization for mass data analysis was proposed for the first time[36] but *in silico* tools for predicting compound classification by fragmentation spectra were not available at that time. Nowadays, with the development of automatic classified *in silico* tools[24], it is time for a revolution of the visualization strategy with higher confidence in classified level.

For above consideration, we proposed a comprehensive framework, named MCnebula, for untargeted LC-MS/MS dataset analysis. MCnebula integrated a new abundance-based classes (ABC) selection algorithm for chemical classes selection. The principle of ABC selection algorithm: (1) applied an initial filtering to thousands of chemical classes based on the predicted probability, (2)regarded all 'features' as a whole, examined the number and abundance of 'features' of each chemical classification (classification at different levels, classification of sub-structure and dominant structure), and then selected representative classes, (3)these chemical classes were followed by goodness assessment (about identification of its classified compounds) and identicality assessment (the extent to which these chemical classes are distinguished from each other in the context of MS/MS spectra). The final chemical classes would serve to the subsequent analysis: visualized as Child-Nebulae and focus on these chemical classes / Nebulae for biomarker or chemistry discovery. The top 'features' based on statistical analysis could be set as tracer to discover more homology compounds of chemical structure or spectral similarity or chemical class. MCnebula can be used to explore unknown compounds because of the annotation module and the cutting-edge technology of SIRIUS software[20,22,34,37–39], which exceeded the limitations of spectral library matching. MCnebula was implemented in the R language and can be easily integrated into the diverse biological analysis workflow of R. MCnebula (updated to MCnebula2, which included more tools such as ABC selection algorithm, Nebula visualization, statistical analysis, and output report etc.) was written primarily in S4 system of object-oriented programming. It allowed all data for one-button analysis from the beginning to the end, which facilitated data processing. In addition to the basic function of MCnebula), we provided an additional 'exMCnebula2' package for downstream analysis, which contained all the analysis tools used in this study such as pathway enrichment analysis, heatmap clustering analysis, spectral visualization analysis, chemical information query, etc. Downstream analysis of untargeted LC/MS-MS is complex and varies from data to data. The additional tools in exMCnebula2 package could provide a prototype for the expanded application of MCnebula.

In this article, two datasets were applied in MCnebula in order to demonstrate the broad utility of our method. One was a human-derived serum dataset that correlated with mortality risk profiling of staphylococcus aureus Bacteremia (SaB); the other was a plant-derived herbal dataset that related to the traditional processing of herbal medicine.

Experimental section

MCnebula algorithm

Overall consideration The analysis of untargeted LC-MS/MS dataset generally begins with feature detection. Features are recognized as "peaks" in MS^1 (MASS level 1) data. Each feature may represent a compound, and assigned with MS^2 (MASS level 2) spectra. The MS^2 spectra was then used to figure out the compound identity. The difficulty was mainly in annotating these features to discover their compound identity and mining out useful information for further biological research. In addition, the untargeted LC-MS/MS dataset was generally a huge dataset, which leads to time-consuming analysis of the whole process. Herein, a classified visualization method, called MCnebula, was used for addressing these issues.

The MCnebula package itself does not involve molecular formula prediction, structure prediction or chemical prediction of compounds, thus the accuracy of these parts was not considered. MCnebula achieved downstream analysis by extracting the prediction data from SIRIUS project. The core of MCnebula was chemical classes filtering algorithm, which was called abundance-based classes (ABC) selection algorithm. To explain the ABC selection algorithm in detail, we need to begin with MS/MS spectral analysis and identify compounds.

Chemical structure and formula. The analysis of MS/MS spectrum was a process of inference and prediction. For example, we speculated the composition of elements based on the molecular weight combined with the possible fragmentation pattern of MS/MS spectrum, we speculated the potential molecular formula of a compound. Finally, we looked for the exact compound from the compound structure database. Sometimes, this process is full of uncertainty, because there were too many factors that could affect the reliability of MS/MS data and the correctness of inference. It can be assumed that there are complex candidates for the potential chemical molecular formula, chemical structure and chemical class behind MS/MS spectrum. Suppose we had these data of candidates now, MCnebula could help extract these candidates and obtain the unique molecular formula and chemical structure for each MS/MS spectrum based on the highest score of chemical structure prediction; in this process, like most algorithms, we can filter the prediction based on score.

Establish reference upon top candidate We predicted a potential compound represented by LC-MS/MS spectrum, and obtained the candidates of chemical molecular formula, structure and chemical class. These candidates include both positive and negative results: for chemical molecular formula and chemical structure, the positive prediction was unique; for chemical class, multiple positive predictions that belonged to various classification were involved. We did not know the exact negative and positive modes. Normally, we ranked and filtered these data by score. There were numerous scores, for isotopes, for mass error, for structural similarity, for chemical classes and so on. Selection of score for ranking candidates depended on the purpose of research. For instance:

- To find out the chemical structure mostly be positive mode, ranking the candidates by structural score.

- To determine whether a potential compound belongs to a certain chemical class, ranking the candidates by the classified score.

By functions in MCnebula of 'filter_formula()', 'filter_structure()' or 'filter_ppcp()', the candidate with top score can be obtained. However, for the three module (formula, structure, classes), sometimes their top score candidates were not in line with each other. That was, their top score towards different chemical molecular formulas. To find out the corresponding data in other modules, 'create_reference()' should be performed to establish the 'specific candidate' as reference for subsequent data integrating.

We obtained the unique chemical molecular formula and chemical structure formula for reference by scoring and ranking. But for chemical classes, such method was not enough.

Chemical classification. Chemical classification is a complex system. Here, we only discuss the structure-based chemo taxonomy system^{24}, because the MS/MS spectrum is more indicative of the structure of compounds than biological activity and other information.

According to the division of the overall structure and local structure of compounds, we can call the structural characteristics as the dominant structure and substructure^{24}. Correspondingly, in the chemical classification system, we can not only classify compounds according to the dominant structure, but also classify according to the substructure. The chemical classification based on the dominant structure of compounds is easy to understand. For example, we will classify Taxifolin as 'Flavones', not 'phenols', although its local structure has a substructure of 'phenol'. We hope to classify a compound by its dominant structure rather than substructure, because such classify is more concise and contains more information. However, in the process of MS/MS spectral analysis, we sometimes can only make chemical classification based on the substructure of compounds, which may be due to: uncertainty in the process of structural analysis; it may be an unknown compound; MS/MS spectral fragment information is insufficient. In this case, it was necessary for us to classify the compounds with the aid of substructure information, otherwise we had no knowledge of the compounds for which we cannot obtain dominant structure information.

We should also be clear about the complexity of another aspect of chemo taxonomy, i.e., the hierarchy of classification. For example, 'Flavones' belongs to its superior, 'Flavonoids'; its next higher level, 'Phynylpropanoids and polyketides'; the further upward classification is 'organic compounds'.

ABC selection. In the untargeted LC-MS/MS dataset, each feature has a corresponding MS/MS spectrum, and there are thousands of features in total. The ABC selection algorithm took all features as a whole, examined the number and abundance of features of each chemical classification (classification at different levels, classification of substructure and dominant structure), and then selected representative classes (mainly screening the classes according to the number or abundance range of features) to serve the subsequent analysis (Fig. 1).

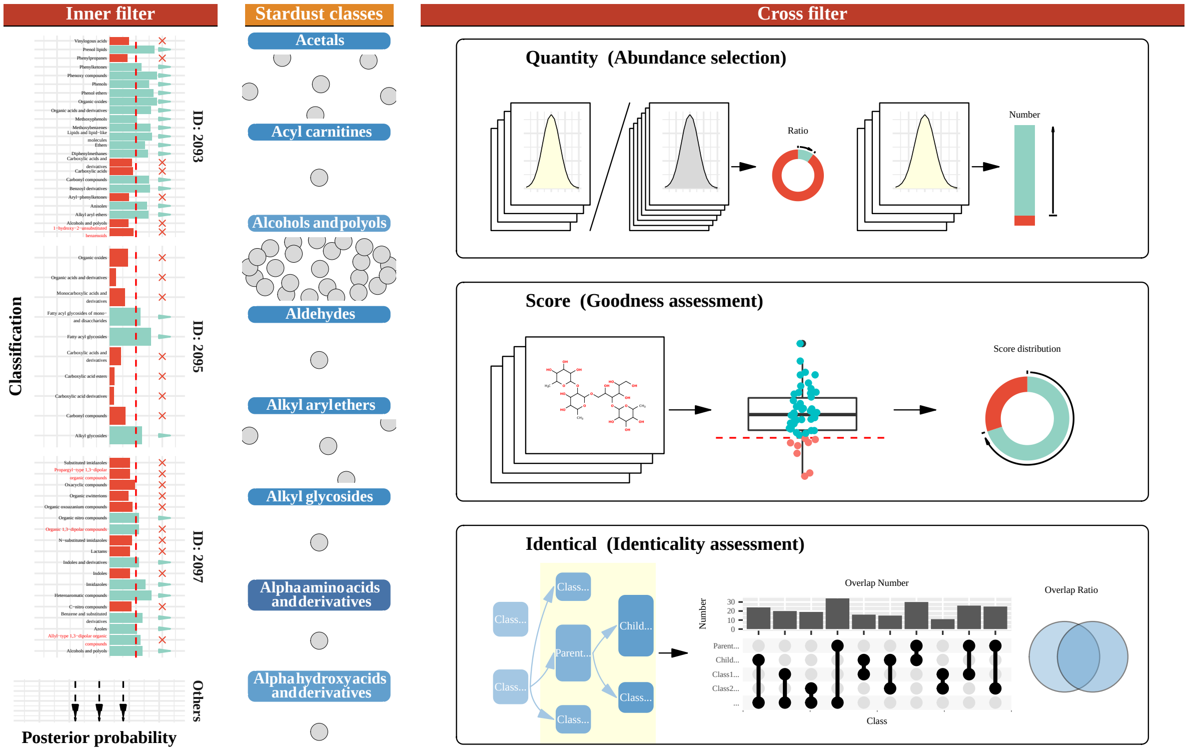

Figure 1: **Mechanism for filtering chemical classes of MCnebula2.** This figure illustrates how MCnebula2 filters chemical classes of prediction from 'features' to form a Nebula-Index to create Child-Nebulae. The **Inner filter** filter out the chemical classes by Regex match of names (names without without Arabic numerals) and set threshold for value of posterior probability. To create **Stardust Classes**, the previous filtered data is re-grouped according to chemical classes instead of 'features' ID. The **Cross filter** conduct further filtering of chemical classes via combining Stardust Classes and 'features' annotation data. The details of Cross filter was described in MCnebula2 Algorithm section in article.

- Create Stardust Classes (Inner filter). The posterior probability of classification prediction (PPCP) data belonged to each 'feature'. When performing the filtering, only simple threshold conditions or absolute conditions were set to filter the chemical classes; there was no crossover between the different attributes and no crossover between the 'features'. Therefore, we considered this as 'inner' filtering.

- Cross filter Stardust Classes. The data of the chemical classes and their classified 'features', i.e. Stardust Classes data, were combined and then grouped upon the chemical classes. After grouping, each chemical class had a certain quantity of 'features'. When filtering, statistics may be performed on 'features' data within a group; statistics may be performed on these data in conjunction with 'features annotation' data; and statistics may be performed to compare groups with each other. As its crossover of attributes for filtering, we consider this as 'cross' filtering. (See details in next subsection about Cross filter Stardust Classes.)

Whether it is all filtered by the algorithm provided by MCnebula function or custom filtered for some chemical classes, we now have a data called Nebula-Index. This data records a number of chemical classes and the 'features' attributed to them. The subsequent analysis process or visualization will be based on it. Each chemical class is considered as a 'nebula' and its classified 'features' are the components of these 'nebulae'. In the visualization, these 'nebulae' will be visualized as networks. Formally, we call these 'nebulae' formed on the basis of Nebula-Index data as Child-Nebulae. In comparison, when we put all the 'features' together to form a large network, then this 'nebula' is called Parent-Nebula.

Details of Cross filter Stardust Classes. This method was an integration of the three modules below (Fig. 1):

Cross filter by 'quantity' (abundance selection). Set 'features' quantity limitation for each group (each group, i.e. a chemical class with its classified 'features'). The groups with too many 'features' or too few 'features' would be filtered out. This means the chemical class would be filtered out. These thresholds are about:

- Minimum quantity: the 'features' within the group.
- Maximum proportion: the 'features' quantity within the group versus all 'features' (unique) quantity of all groups.

The purpose of this step is to filter out the chemical classes that have too large or too subtle a conceptual scope. For example, 'Organic compounds', which covers almost all compounds that can be detected in metabolomics data, is too large in scope to be of any help to our biological research. The setting of parameters is not absolute, and there is no optimal solution. Users can draw up thresholds according to the necessity of the study.

Cross filter by 'score' (Goodness assessment). This step associate Stardust Classes data with 'features' annotation data. For each group, the Goodness assessment is performed for each target attribute (continuous attribute, generally be a scoring attribute of compound identification, such as 'Tanimoto similarity'). If the group met all the expected Goodness, the chemical class would be retained; otherwise, the chemical class would be filtered out. The Goodness (G) related with the 'features' within the group:

- n: the quantity of 'features' of which target attributes satisfied with the cut-off.
- N: the quantity of all 'features'.

The Goodness: $G = n/N$.

The assessment of Goodness is related to the parameters of 'tolerance' and 'cutoff':

- Expected Goodness, i.e. value of 'tolerance'.
- Actual Goodness, related to parameter 'cutoff'. $G = n/N$.

Goodness assessment can be given to plural target attributes. Note that the chemical class would be retained only if it passed the Goodness assessment of all target attributes. The main purpose of this step is to filter out those chemical classes with too many 'features' of low structural identification.

Cross filter by 'identical' (identicality assessment). A similarity assessment of chemical classes. Set a hierarchical range for chemical classification and let groups within this range be compared for similarity to each other. For two groups, if the classified 'features' are almost identical to each other, the chemical class represented by one of the groups would be excluded. The assessment of identical degree of two groups (A and B):

- x: ratio of the classified 'features' of A belonging to B
- y: ratio of the classified 'features' of B belonging to A
- i: value of parameter 'identical_factor'

If $x > i$ and $y > i$, the two groups would be considered as identical. Then the group with fewer 'features' would be discarded. The purpose of this step is to filter out classes that may incorporate each other and are similar in scope. The *in silico* prediection approach may not be able to distinguish which class the potential compound belongs to from the LC-MS/MS spectra.

Network graph presentation As mentioned above, 'features' and their annotations were integrated as Nebulae according to the Nebula-Index. These Nebulae were network-type graph data. The 'features' annotation data contains top candidate of chemical formula and structure (obtained with the MCnebula function 'filter_*()'). The MS/MS spectral similarity (dot product) of the 'features' was calculated and used to form the edge data for the network graph.

Visualization system MCnebula used a number of existing R packages to integrate and reformat data. In particular, the network graph data was equipped with 'ggplot2' package for visualization. The ggplot2 package is known for its elaborate and aesthetic mapping characteristics. We designed the 'ggset' data class to store pre-defined ggplot2 plotting functions and parameters for visualizing Nebulae. This allows users to completely customize the visualization to suit their needs or the needs of the publisher. Its flexibility depends on the user's understanding and proficiency of the 'ggplot2' package. If users are not experienced in using the 'ggplot2' package, he should just follow the preset package for visualization.

Statistic analysis MCnebula integrated the functions (mainly for: 'limma::makeContrasts', 'limma::lmFit', 'limma::lmFit', 'limma::eBayes') of the 'limma' package for differential expression analysis (analysis of RNA-sequence and microarray) and packaged them for differential analysis of metabolomics data[40]. The gene expression matrix and the feature quantification matrix of LC-MS are similar, both of which have corresponding explanatory variables (sample information) and dependent variables (gene expression values or feature quantification values), except that one represents the level of gene expression and the other the level of metabolite. We normalized the peak area levels of the features and transformed (log2) them, used the metadata information of the samples to create the design matrix and the contrast matrix[40]; thus even if the data itself is not gene related, it can be performed differential analysis using the tools of the 'limma' package. The 'limma' is a powerful package for differential analysis using linear models that can handle not only simple experimental designs in which the explanatory variables are factors (e.g., Control group versus Model group), but also complex experimental designs in which the explanatory variables are covariates (e.g., groups containing time series). However, our packaged method was only appropriate to experimental designs in which explanatory variables are factorial variables and the design matrix without intercept (code: 'model.matrix(~ 0 + group)')[41]. Because of its simple applicability, we called it 'binary comparison'. Our evaluation section does not cover its evaluation (as it is not the main part of this study), but we used it in two demo datasets and validated them to some extent: in the serum dataset, we compared our obtained top 'features' with that of Wozniak et al.[42]; in the herbal dataset, we traced the obtained top 'features' to the EIC plot.

Data structure MCnebula was written mainly in R S4 system of object-oriented programming. When we analyzed data with MCnebula, all data (whether 'features' annotation data or visualization data) was stored in a one object (class 'mcnebula'). This reduced the difficulty of using the MCnebula package, and made the data easy to manage and the analysis easy to repeat.

Report system MCnebula integrated a reporting system that allows the analysis process to be output as a PDF document or in other formats. The reporting system was based on the data class 'report', which could stores each step of the analysis as a section and could be flexibly modified according to the user's needs. In addition, the reporting system can be used to generate reports even if the analysis is completely irrelevant to MCnebula package. The reporting system was associated with the 'rmarkdown' R package[43].

Code Compatibility MCnebula conducted downstream analysis by extracting the data from the already computed SIRIUS project. The SIRIUS project is the main source of data for MCnebula 2. The SIRIUS software is still being updated and improved. In fact, from SIRIUS version 4 to version 5 (https://github.com/boecker-lab/sirius), the data structure and attributes name in the project directory have changed. In order that the functionality of MCnebula is not invalidated due to versioning issues, its application program interface (API) for the SIRIUS project has been designed to be flexible. MCnebula is able to perform data extraction for different SIRIUS versions.

MCnebula evaluation

Spectra dataset for evaluation. The spectra collection (in positive ion mode, for more spectra data) of GNPS MS/MS library was used for evaluation (.msp file) (http://prime.psc.riken.jp/compms/msdial/main.html#MSP). As Fragmentation spectra in reference library generally possess high quality, and while used for evaluation of library match, it may cause overfitting. To address the issue, refer to ref.[44], we added 'noise' into these MS/MS spectra. In brief, the 'noise' involves mass shift, intensity shift, and the inserted noise peak; of note, the magnitude factors for these shift were drawn randomly from function of normal distribution. Overall, we simulated two model of 'noise' (medium noise and high noise). The 'noise' simulation was achieved in custom R script. These algorithms and parameters were parallel to the reference[44]. We assigned these datasets as origin dataset, medium noise dataset and high noise dataset. The details of simulation of noise were as following:

- A global mass shift was simulated by drawing a random number δ^* from $N\left(0, \sigma_{mb}^2\right)$ (Normal distribution) and then shifting every peak mass m by $\delta^* m$. The standard deviation σ_{mb} was chosen as

$\sigma_{mb} = (10/3) \times 10^{-6}$ (medium noise) or $\sigma_{mb} = (15/3) \times 10^{-6}$ (high noise), so that the $3\sigma_{mb}$ interval represents a 10-ppm shift for medium noise and a 15-ppm shift for high noise.

- Individual mass deviations was simulated by drawing, for each peak with mass m individually, a random number δ from $N\left(0, \sigma_{md}^2\right)$ and shifting the peak by δm. The standard deviation σ_{md} was chosen so that the $3\sigma_{md}$ interval represents a 10-ppm shift for medium noise and a 20-ppm shift for high noise.
- Intensity variations were simulated in the spectrum. Each peak intensity was multiplied by an individual random number ϵ drawn from $N\left(1, \sigma_{id}^2\right)$. Variance was chosen as $\sigma_{id}^2 = 1$ for medium noise and $\sigma_{id}^2 = 2$ for high noise. 0.03 times the maximum peak intensity of the spectrum was subtracted from each peak intensity. If a peak intensity fell below the threshold of one thousands of the maximum intensity in the spectrum, the peak was discarded.
- Additional 'noise peaks' were added to the spectrum. In processing of origin dataset, a pool of 'noise peaks' was gathered from the fragmentation spectra, using all peaks that did not have a molecular sub-formula decomposition of the known molecular formula of the precursor. For each spectrum, αn of these 'noise peaks' were added to the spectrum, where n is the number of peaks in the spectrum and $\alpha = 0.2$ for medium noise and $\alpha = 0.4$ for high noise. Intensities of 'noise peaks' were adjusted for maximum peak intensities in the contributing and receiving spectrum. 'Noise peaks' were randomly drew from the pool of 'noise peaks' and added to the spectrum.

For another issue, the spectra collection did not possess isotopes pattern. In real LC-MS processing (feature detection), isotope peaks were grouped and merged, which favorable for SIRIUS to detect some specific element[37]. To simulate isotopes pattern, we used function of 'get.isotopes.pattern' within 'rcdk' R package to get isotope mass and its abundance[45]. Furthermore, these mass were considered for the adduct type to increase or decrease exact mass. For the 'intensity' of these isotope pattern, we simulated as relative intensity, i.e., the abundance of isotopes multiply by 100 by value. These 'isotope peaks' were merged into MS^1 list of its compounds. All the spectra collections were formatted to fit with input of MCnebula workflow or benchmark method (.mgf file and feature quantified table .csv).

Evaluation method. The three simulated data were all run with MCnebula workflow and benchmark method. While these data were put into SIRIUS 4 command-line interface (CLI) (version 4.9.12) for computation, the MS/MS spectra with empty fragmentation peak were auto-filtered. In addition, to reduce computation time, the compounds with over 800 m/z precursor were filtered out manually. These filtered out compounds were excluded from ultimate accuracy assessment. There were 8782 MS/MS spectra within the raw collection, and after filtered or excluded, totally 7524 compounds for ultimate evaluation.

The assessment of classified accuracy was conducted with the help of ClassyFire[24]. In detail, we traversed the raw .msp spectra file to collate metadata of these compounds, involving structure annotation. The International Chemical Identifier Key (InChIKey) of these compounds were available for ClassyFire database retrieve. However, since ClassyFire only support those chemical identity of which structure have been classified in its server previously, we noticed all the InChIKeys were vetoed. To address that, we employed first hash block of these InChIKeys (InChIKey planar, represent molecular skeleton) to touch PubChem application programming interface (API) (https://pubchemdocs.ncbi.nlm.nih.gov/pug-rest)[46]. Accordingly, we got all the possibly InChIKeys of isomerism (stereo, isotopic substitution)[47]. The classification of small molecules depends on its molecular skeleton hence these chemical identities possess the same InChIKey planar are identical in classification. We pushed the obtained InChIKey list to ClassyFire to obtain classification. In R script, once any InChIKey of isomerism meet the classified data in database, the acquisition status for this molecular skeleton was turned off. In the end, all these chemical annotation were collated, integrated and assigned as standard reference.

The discrepancies between the MCnebula and benchmark methods in terms of algorithm and classified results disallow them to be evaluated at completely the same level. We evaluated both methods respectively. For MCnebula, before assess the accuracy, we interrogated the obtained classes generated from pre-analysis of the origin dataset. The classes over in half were classified based on sub-structural class, such as 'Organic carbonic acids and derivatives', 'Hydroxy acids and derivatives'. These classes were small in structural size and were chemical function group within compounds. The principle of ClassyFire is selecting the most dominant structural class of compounds to substitute[24]. But, in perspective of drug discovery, structure determines potency; many pharmacological action possibly depends on these sub-structure. To locate more universality among features, in algorithm, we reserved these classes in results. Sub-structural classify for benchmark method not available, hence we neglected these classes in evaluation. The rest classes, nevertheless, still possibly be sub-structural class while meet some compounds. We assigned three levels for evaluation, i.e., 'True', 'Latent', 'False'. The 'True' indicated the classified classes were in line with that of ClassyFire. The 'Latent' indicated the classified classes were not in line with that of ClassyFire, but their parent classes of 'class' level were in line with that of ClassyFire. The 'False' indicated the classified classes were completely inconsistent with that of ClassyFire.

To assess the identification of classes or structures, the results were merge with standard reference by InChIKey planar. For assessment of identification of chemical structure, once the identified chemical structure was in line with or chemical structure (match by InChIKey planar), we assigned it as 'true'. Indeed, such evaluation neglect stereochemistry.

Serum dataset

We re-analyzed 245 LC-MS/MS data (.mzML) from MASSIVE (id no. MSV000083593) (blanks, controls and samples)[42]. MZmine2 (version 2.53) was performed for feature detection. The detection workflow mainly involves **1)** Automated Data Analysis Pipeline (ADAP) for peak detection and deconvolution[9], **2)** isotopes peak finder, **4)** parallel samples join alignment, **5)** gap filling algorithm. While we exported MS/MS spectra (.mgf) for SIRIUS 4 software computation, spectra were merged across samples into one fragmentation list with 30% Peak Count threshold filtering. The feature detection workflow was referred to FBMN preprocessing and SIRIUS computational prerequisites. The output .mgf was run with SIRIUS 4 software (version 4.9.12) for computation with SIRIUS[22], ZODIAC[39], CSI:fingerID[20], CANOPUS[34]. In particular, SIRIUS was customized set to detect Iodine element while predicting formula. MCnebula package were used for subsequent data analysis. All subsequent analysis have been organized into concise code and exported as reports (see section of Data and code availability).

Kyoto Encyclopedia of Genes and Genomes (KEGG) metabolic pathway enrichment analysis was performed with 'Lysophosphatidylcholines' (LPCs) and 'Bile acids, alcohols and derivatives' (BAs), respectively. We used the identified InChIKey planar of structures to hit compounds in metabolic pathway. In detail, firstly, in order to avoid the identified structural deviations due to stereoisomerism, the InChIKey planar was used to obtain all possible InChIKeys via PubChem API. In this step, PubChem CID of those compounds were also obtained. The R package of MetaboAnalystR was used for converting PubChem CID to KEGG ID[48]. Many compounds were not related to metabolic pathway so those were filtered out. The R package of FELLA was used for KEGG enrichment with 'pagerank' algorithm[49]. The above methods have been integrated as functions to interface with the MCnebula workflow. These functions are available in the 'exMCnebula2' package.

Herbal dataset

Material and processing. *E. ulmoides* dried bark was obtained from company of ZheJiang ZuoLi Chinese Medical Pieces LTD. Raw-Eucommia and Pro-Eucommia were prepared as followed: (1) Raw-Eucommia: The shreds or blocks of *E. ulmoides* dried bark were took, powdered and passed through 80-mesh sieves for further process. (2) Pro-Eucommia: The shreds or blocks of *E. ulmoides* dried bark were sprayed with saline water (the amount of salt is 2% of *E. ulmoides*, add 10 fold of water to dissolve), and smothered in airtight for 30 min. Then, the barks were dried in oven at 60 °C, followed by baking at 140 °C for 60 min. Finally, the baked barks were powdered and passed through 80-mesh sieves for further process.

Sample preparation. 2 g of Raw-Eucommia powder and Pro-Eucommia powder were weighed, respectively, added 50 ml of methanol/water (1:1, v/v) followed by ultrasonic (20 kHz for 40 min). After ultrasonic, the mixture was filtered to obtain filtrate and residue. The residue was added with 50 ml of methanol/water (1:1, v/v) and extracted with ultrasonic (40 kHz, 250 W for 20 min) again. The mixture was filtered. Then, the filtrate of the two extracts was combined, the solvent was evaporated. Methanol/water (1:1, v/v) was added to redissolve the extract and the volume was fixed to 5 ml. Finally, the supernatant was obtained by centrifugation (12,000 r.p.m. for 10 min) for further LC−MS analysis.

LC-MS experiments. LC−MS analysis was performed using a Dionex Ultimate 3000 UHPLC system (Dionex, Germany) coupled with a high-resolution Fourier-transform mass spectrometer (Orbitrap Elite, Thermo Fisher Scientific, Germany) using a Waters Acquity HSS T3 column (1.8 mum, 100 mm × 2.1 mm, Waters Corporation, Milford, MA, USA). Solvent A, formic acid/water (0.1:99, v/v), and solvent B, formic acid/acetonitrile (0.1:99, v/v), were used as the mobile phase. The gradient profile for separation was as follows: 2% of solvent B at 0min, 5% of solvent B at 2 min, 15% of solvent B at 10 min, 25% of solvent B at 15 min, 50% of solvent B at 18 min, 100% of solvent B at 23 min, 2% of solvent B at 25 min, and 2% of solvent B at 30 min. The flow rate was 0.3 ml/min. The column temperature was set at 40°C. Mass spectrometric analysis was performed using an Orbitrap Elite instrument equipped with an ESI source (Thermo FisherScientific, Germany) that operated in the negative ionization mode. The ESI source was operated at 50 °C with a capillary temperature of 275 °C, an ionization voltage of 3.5 kV, and a sheath gas flow rate of 35 L/min. The survey scans were conducted in the Orbitrap mass analyzer operating at a 120,000 (full width at half-maximum) resolving power. A mass range of 100−1500 m/z and a normalized collision energy of 30 eV were used for survey scans. The analysis method was set to analyze the top 10 most intense ions from the survey scan, and a dynamic exclusion was enabled for 15 s.

MCnebula Workflow. E.ulmoides dataset was preprocessed with MZmine2 for feature detection, followed by SIRIUS software computation. The subsequent analysis was similar to serum metabolic dataset and also been organized as a report (see section of Data and code availability).

Data processing

Raw data (.raw) were converted to m/z extensible markup language (mzML, i.e., .mzml format data) in centroid mode using MSConvert ProteoWizard[5]. The .mzml files were processed with MZmine2 (v.2.53) and followed by SIRIUS 4 in Pop!-OS (Ubuntu) 22.04 LTS 64-bits workstation (Intel Core i9-10900X, 3.70GHz × 20, 125.5 Gb of RAM)[8]. MCnebula (MCnebula2) and other R packages were executed in Pop!_OS (Ubuntu) 22.04 LTS 64-bits PC (Intel Core i7-1065G7, 1.3 GHz × 8, 16 Gb of RAM).

Data and code availability

The source code of MCnebula was available at https://github.com/Cao-lab-zcmu/MCnebula. The source code of exMCnebula2 was available at https://github.com/Cao-lab-zcmu/exMCnebula2. The code for all the analysis in this study can be found in the internal data directory ('inst/extdata/') of the 'exMCnebula2' package. In addition, .mgf files (msms spectra) and .csv files (feature quantification) and SIRIUS output files (use MCnebula function to filter and compress tens of GB of data to just a few tens of MB) and analysis report of serum and herbal dataset were compressed and stored in the exMCnebula2 package. By downloading and installing MCnebula package and exMCnebula2 package, all the analyses of this study can be reproduced by executing R codes.

The serum dataset were available at MassIVE web service (id no. MSV000083593). The submission job in GNPS of evaluation dataset are available: 1) original dataset: FBMN: https://gnps.ucsd.edu/ProteoSAFe/status.jsp?task=05f492249df5413ba72a1def76ca973d. MolnetEnhancer: https://gnps.ucsd.edu/ProteoSAFe/status.jsp?task=9d9c7f83fa2046c2bf615a3dbe35ca62; 2) medium noise dataset: FBMN: https://gnps.ucsd.edu/ProteoSAFe/status.jsp?task=c65abe76cd9846c99f1ae47ddbd34927; MolnetEnhancer: https://gnps.ucsd.edu/ProteoSAFe/status.jsp?task=7cc8b5a2476f4d4e90256ec0a0f94ca7; 3) high noise dataset: FBMN: https://gnps.ucsd.edu/ProteoSAFe/status.jsp?task=62b25cf2dcf041d3a8b5593fdbf5ac5e; MolnetEnhancer: https://gnps.ucsd.edu/ProteoSAFe/status.jsp?task=f6d08a335e814c5eac7c97598b26fb80.

Results and discussion

Results

Overview The MCnebula workflow was dedicated to analyzing LC-MS/MS datasets from the beginning, i.e. starting from the raw data obtained from the sample and going through the various stages of analysis to obtain a complete analysis report (Fig. 2). The analysis process followed the general MCnebula analysis templates, from filtering candidates of chemical formula, structural formulae, chemical classes, to creating visual Nebulae; it also allowed for custom advanced analysis, with the help of chemical class focused Nebulae, to perform statistic analysis, features selection, focus on critical metabolites (compounds) and their structural characteristics, pathway enrichment, querying compound synonyms, etc. We evaluated workflow of MCnebula in function with other popular public available methods. In terms of the evaluation of our chosen indicators which cover identification, classifying, etc., MCnebula has a wider scope of applicability. (Tab. S1)

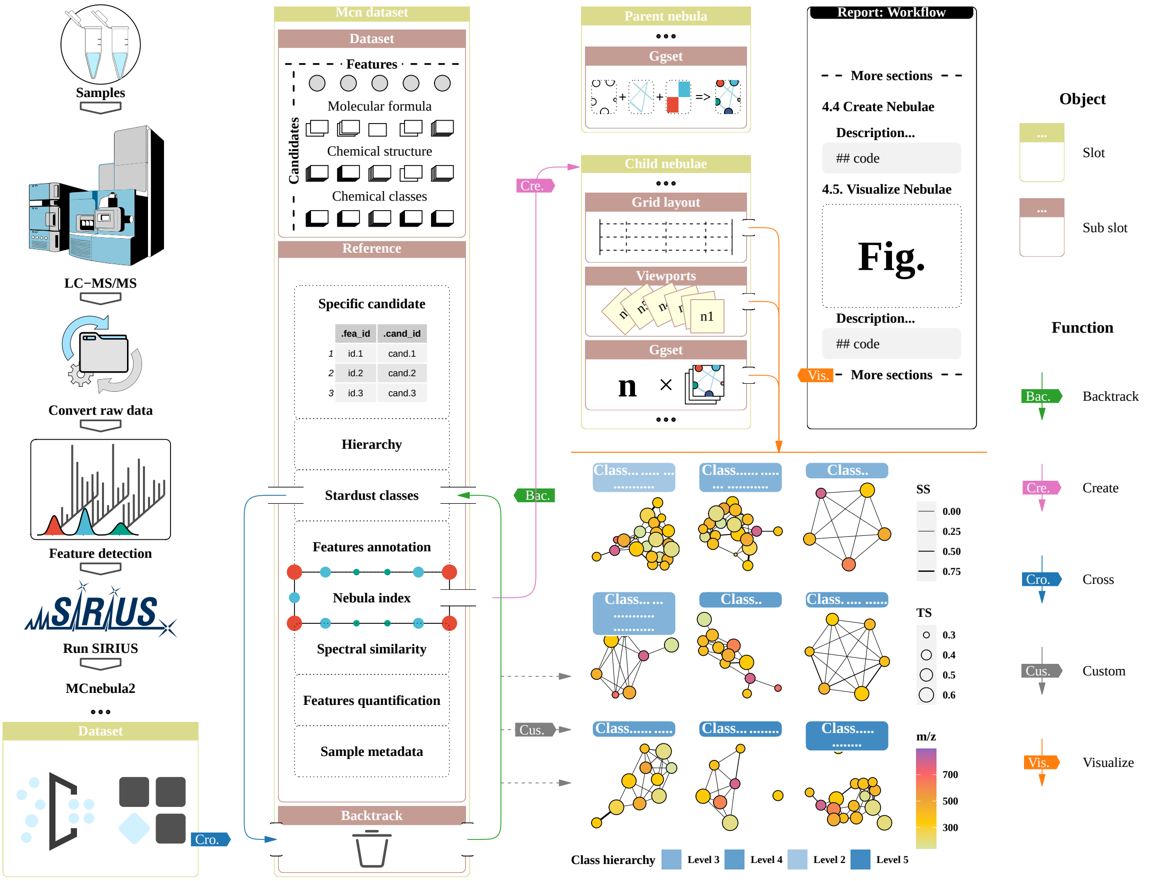

Figure 2: **Data stream of MCnebula workflow.** The MCnebula workflow can be divided into two parts, depending on the platform on which the data presents. The first is the part beyond R (before MCnebula2): from the **Samples** to **LC-MS/MS** to obtain the raw data; the stage of **Convert raw data** is implemented using the popular MSconvert tool derived from Proteowizard; for **Feature detection**, users can implement it with any LC-MS processing tool, such as MZmine, XCMS, OpenMS, etc.; then .mgf or other file format of MS/MS spectra is imported into SIRIUS for computations. The part inside R, MCnebula2 implements integrating data and creating Nebulae within 'mcnebula' object (see section of MCnebula2 algorithm in article for details).

Method evaluation **Classified accuracy.** We used a public available reference spectral library to assess the accuracy of classifying by MCnebula. The direct use of such a reference spectral library may lead to overfitting during the evaluation. We have taken the approach of simulating noise to eliminate this consequence. Simulating noise, i.e., adding invalid noisy data to the reference spectrum or numerically shifting the existing data, also simulates data acquisition similar to a real scenario: due to the different acquisition conditions, the spectral data in the real case will be more noisy compared to the reference spectrum. By adding noise to the reference spectral library, we now have three datasets for evaluation (origin, medium noise and high noise dataset) (commonly 7524 compounds (spectra)). All three datasets were analyzed using MCnebula. Due to the richness of the compounds in the reference spectra, for the origin dataset, we obtained a total of 152 chemical classes (each with a corresponding compound to be evaluated) via using ABC selection algorithm. These 152 chemical classes include both chemical classes refined on the basis of dominant structures and chemical classes refined on the basis of substructures. To facilitate comparison with other methods, we selected only chemical classes that are likely to be dominant structures for evaluation. There were 37 such chemical classes that were selected for evaluation. To evaluate MCnebula more objectively, we chose the molecular networking provided by GNPS (Global Natural Products Social Molecular Networking), with the modules of Feature-based molecular networking (FBMN) and MolNetEnhancer, as the benchmark method to provide a visualized clustering analysis of mass spectra data. GNPS is a typical and popular spectral library-based mass spectrometry annotation method. In principle, it first calculates spectral similarity by conducting mirror match with public spectral library, identifies compounds with the exact chemical structures, and then determines the chemical class based on the annotated chemical structure.

We uploaded the three datasets to the GNPS server and then obtained the results and used them for evaluation. For origin dataset, GNPS resulted in a total of 44 chemical classes (parallel to MCnebula, with at least 50 compounds per chemical class). There were 19 common classes in total. These classes were selected to compare MCnebula and GNPS in parallel in terms of classified number, stability, and relative false rate. For the classified number, MCnebula outperformed GNPS in three datasets (MCnebula: 199, 178, 160; GNPS: 162, 95, 81) (Fig. 3a). For the stability of the classifying after adding noise, MCnebula outperformed GNPS in two dataset (MCnebula: 10.5%, 19.8%; GNPS: 41.7%, 50.1%) (Fig. 2a). For the last indicator, to assess the performance of classifying, it combined the level of the stability to calculate the relative false rate, rather than the absolute false rate. The relative false rate better simulated the actual application to LC-MS/MS analysis, since the actual spectral data contains not only noise but also many unknown compounds that cannot be identified by spectral matching. In this context, MCnebula outperformed the GNPS in the evaluation of the relative false rate in three datasets (MCnebula: 30.2%, 32.9%, 32.6%; GNPS: 51.9%, 48.8%, 47.6%) (Fig. 3a). In addition to the three indicators mentioned above, we also compared MCnebula and GNPS at the individual level for the 19 chemical classes (Fig. 3b). Remarkably, MCnebula was more stable to noise than GNPS.

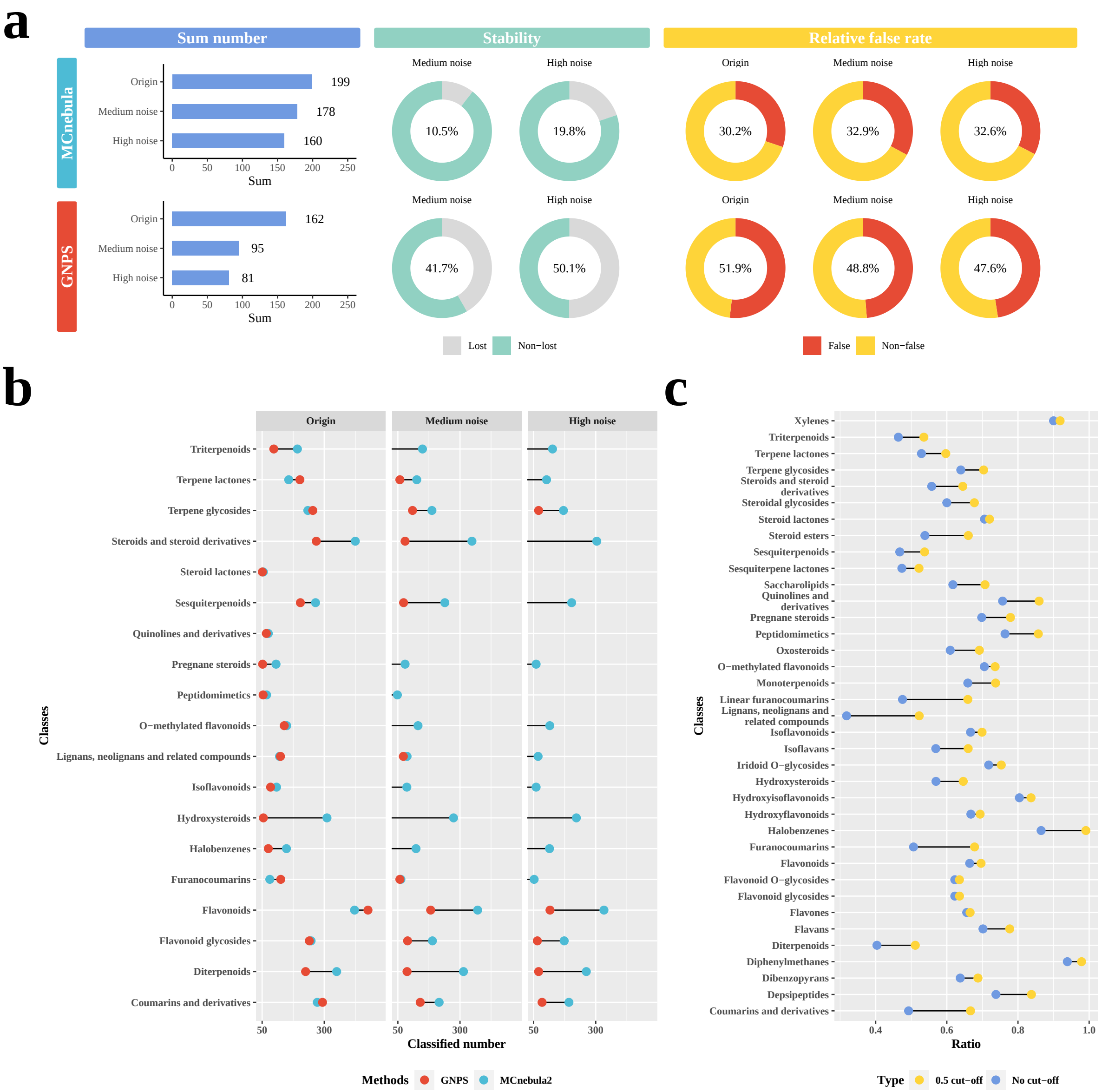

Figure 3: **Comparison of classifying of MCnebula with benchmark method and Evaluation of identification accuracy of MCnebula**. **a)** Fig. 3a illustrates the comparison of MCnebula and benchmark method (GNPS) with three indicators: classified number, stability, relative false rate. The classified number is calculated as average sum number of classified compounds of the selected 19 chemical classes. The stability is calculated as: $S = (N_{origin} - N_x)/N_{origin}$ (N_{origin} is the average sum number of origin dataset; N_x is the average sum number of medium noise dataset or high noise dataset). The relative false rate is calculated as: $R = 1 - (1 - F) \times (1 - S)$ (F is the absolute false rate; S is the stability, i.e., the average - lost rate in stability assessment). **b)** Fig. 3b illustrates a comparison of classified number of MCnebula and benchmark method. When noise is added into original dataset, some number of classified features are occurred < 50, a cut-off (number ≥ 50) is set to exclude these classes from assessment. **c)** Fig. 3b illustrates the identified accuracy of MCnebula. A cut-off (Tanimoto similarity ≥ 0.5) is set to get chemical structures of high matching score for evaluation.

Identified accuracy. Using MCnebula workflow, the origin dataset containing 8057 compounds (precursor ions m/z < 800), all of these compounds were predicted with chemical molecular formulae, and of these, 6610 compounds were predicted with chemical structure. Those chemical structure were evaluated for accuracy in a classified context. For the 37 chemical classes (Fig. 3c), the average false rate of identification was 37%; the average identified compounds number was 156. Among them, most of the identified false rate were between 30% to 40%, however, some classes were quite low, such as ‘Long-chain fatty acids’ or ‘Lignans, neolignans and related compounds’. The reliability of the predicted chemical structure can be assessed in terms of a score. Tanimoto similarity provides such a score for each predicted chemical structure (it provides the matching degree of chemical fingerprints with structures). When Tanimoto similarity sets the cutoff value to 0.5, the average false rate of identification was 29.4%; the average identified compounds number was 139 (Fig. 3c). Above we evaluated the accuracy of the identification of compounds in each chemical class obtained by MCnebula. It should be noted that MCnebula itself does not contain any module for identification, it only utilized the top scoring candidate from the SIRIUS predicted results for annotation. For more evaluation on identification please refer to the publication and our previous related work[22,50].

Data analysis **Serum metabolic analysis.** To illustrate the application of MCnebula in metabolism, we re-analyzed the serum data from Wozniak et al.[42]. The serum samples were collected from patients in-hospital infected with Staphylococcus aureus bacteremia (SaB) or not and healthy volunteers. Overall, the samples were divided into 1) control groups, involving NN (non-hospital, non-infected) and HN (hospital, non-infected); 2) infection groups, involving HS (hospital, survival), HM (hospital, mortality).

A total of 7680 ‘features’ were detected while running with LC-MS preprocessing on the serum dataset. After predicting the compounds by MS/MS spectra (with SIRIUS software), subsequent analysis was performed using MCnebula. Of these, 6501 ‘features’ were annotated with predicted molecular formula and further, 3449 ‘features’ were annotated with predicted chemical structure. Using ABC selection algorithm, we filtered out more than one thousand chemical classes by applied of ‘inner filter’ module (see method section of ABC selection algorithm); further filtered out 508 chemical classes while performing ‘cross filter’; for the remaining 41 chemical classes, 19 chemical classes were manually filtered out, while leaving the final 22 chemical classes to make up the Nebula-Index, which further visualized as Child-Nebulae. It is worth mentioning that the filtered out 527 (508 + 19) chemical classes could be re-added to the analysis. Herein, with the basic workflow of MCnebula, Parent-Nebula and Child-Nebulae were obtained (Fig. S1, Fig. S2). By interrogating Child-Nebulae, we had a basic insight into the chemical classes contained in the serum dataset. To mine more information from Child-Nebulae: we performed a binary comparison of HS and HM groups, ranking ‘features’ according to Q-value (adjusted P-value); the top 50 ‘features’ were set as ‘tracers’ to mark them in Child-Nebulae (Fig. 4). By combining the features selection algorithm about Q-value, the chemical classes exhibited in Child-Nebulae were reduced. The log2(Fold Change) (log2(FC)) quantification for the HM versus HS groups was visualized in Child-Nebulae (Fig. S3). In Fig. S3, the overall level of ‘Bile acids, alcohols and derivatives’ (BAs) class and ‘Acyl carnitines’ (ACs) (Fig. 5a and b) class increased remarkably, while the overall level of ‘Lysophosphatidylcholines’ (LPCs) class decreased remarkably. Indeed, BAs, ACs and LPCs were reported associated with liver dysfunction, imbalance of intestinal microphylactic homeostasis, and mortality risk[42,51,52].

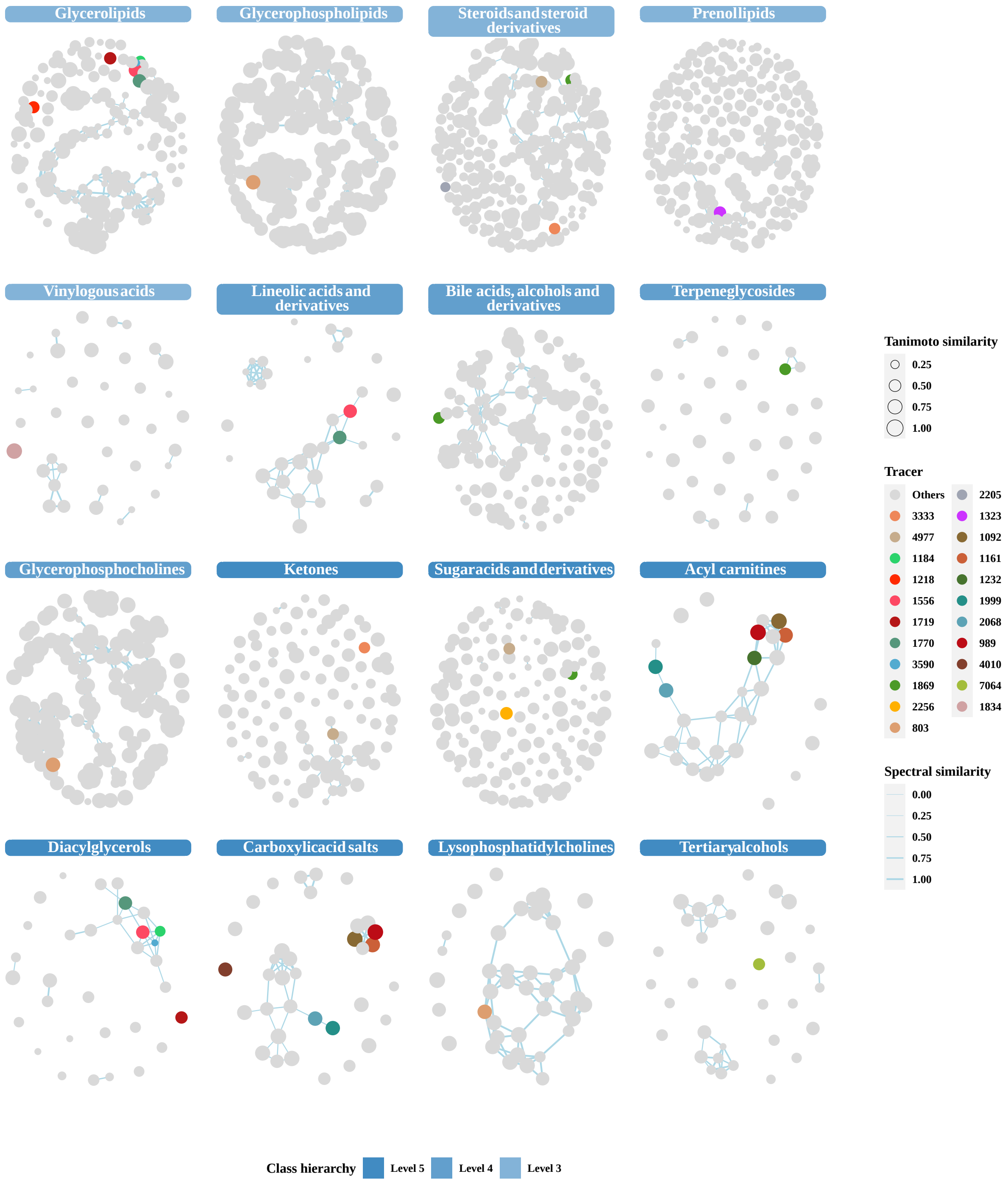

Figure 4: **Tracing top 'features' in Child-Nebulae of serum metabolomics dataset.** According to the rankings of 'features' by statistic analysis, the top 'features' are marked with different colors in Child-Nebulae.

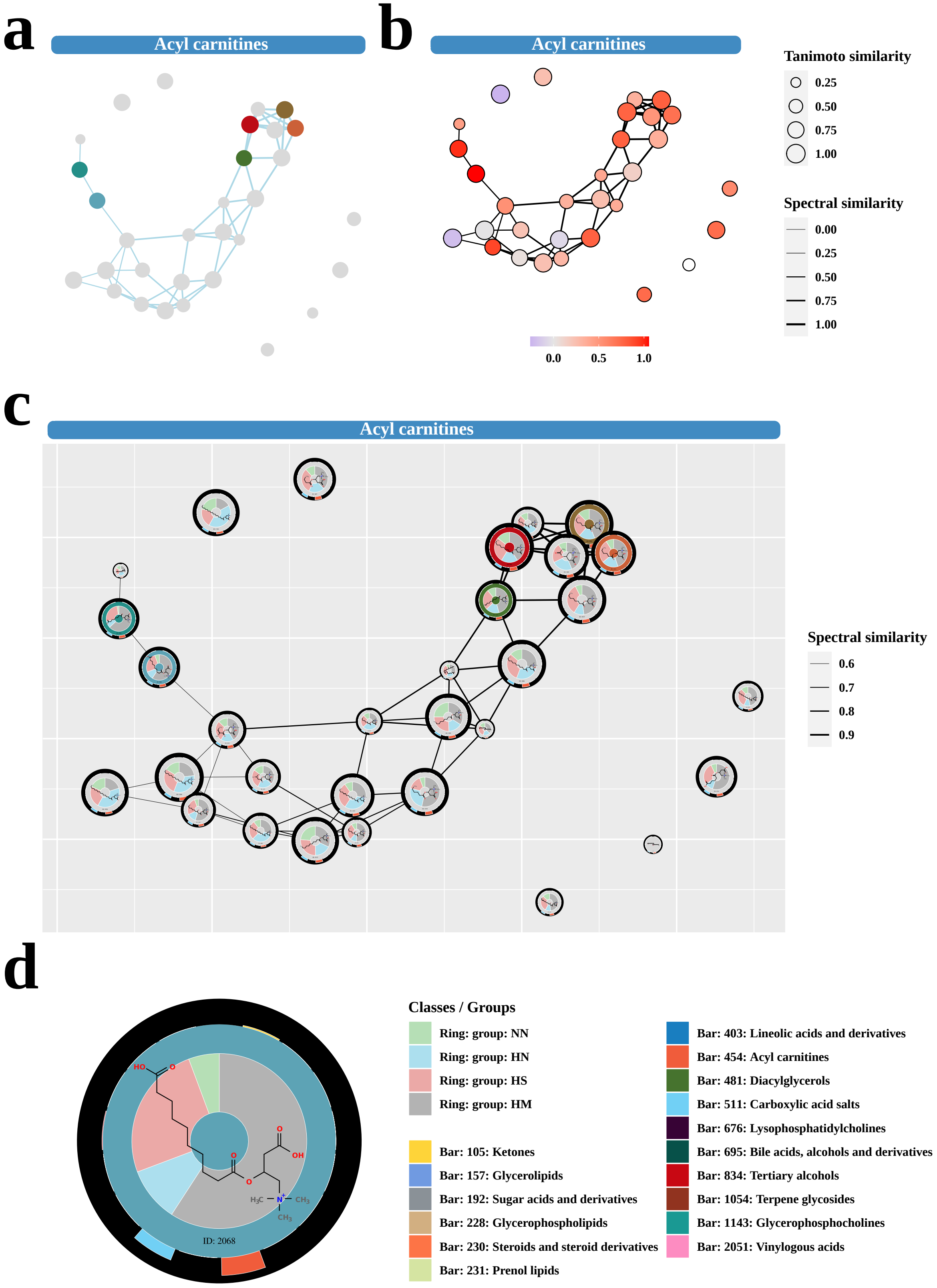
a
Acyl carnitines
b
Acyl carnitines
Tanimoto similarity
0.25
0.50
0.75
1.00
Spectral similarity
0.00
0.25
0.50
0.75
1.00
0.0
0.5
1.0
c
Acyl carnitines
Spectral similarity
0.6
0.7
0.8
0.9
d
HO
O
O
O
OH
H3C
N+
CH3
CH3
ID: 2068
Classes / Groups
Ring: group: NN
Ring: group: HN
Ring: group: HS
Ring: group: HM
Bar: 105: Ketones
Bar: 157: Glycerolipids
Bar: 192: Sugar acids and derivatives
Bar: 228: Glycerophospholipids
Bar: 230: Steroids and steroid derivatives
Bar: 231: Prenol lipids
Bar: 403: Lineolic acids and derivatives
Bar: 454: Acyl carnitines
Bar: 481: Diacylglycerols
Bar: 511: Carboxylic acid salts
Bar: 676: Lysophosphatidylcholines
Bar: 695: Bile acids, alcohols and derivatives
Bar: 834: Tertiary alcohols
Bar: 1054: Terpene glycosides
Bar: 1143: Glycerophosphocholines
Bar: 2051: Vinylogous acids

Figure 5: **In-depth visualization of Child-Nebula of 'Acyl carnitines' a)**, refer to Fig. 4. **b)** The $\log_2$(Fold change) value of HM versus HS group is shown in Child-Nebulae as gradient color. The nodes with white color indicate 'features' with missing quantification value (these 'features' were detected in our re-analysis, but not in Wozniak et al.). **c)** The nodes of top 'features' are marked with color. The nodes of 'features' are annotated with structures, ring diagram and bar plot of posterior probability of classes prediction (PPCP). The top candidate of Chemical structure of 'features' are mapped into nodes. The Ring diagram map relative summed peak area of per 'feature' detected within each metadata group (NN: non-hospital, non-infected; HN: hospital, non-infected; HS: hospital, survival; HM: hospital, mortality). The nodes without ring diagram indicate 'features' with missing quantification value (these 'features' were detected in our re-analysis, but not in Wozniak et al.) The Bar plot map PPCP of structural (sub-structural or dominant structural) classes for the 'feature'. **d)** The zoom in node of 'feature' 2068 (ID) and its legend.

By deep annotation of Child-Nebula, all three classes of compounds have similar structural parent nuclei, and their levels in the NN, HN, HS, and HM groups are similar (Fig. 5c, Fig. S4). Subsequently, we performed cluster heat map analysis and pathway enrichment analysis on the compounds of these three classes. As shown in the clustering heat map (Fig. 6), the control group of ACs and BAs were remarkably separated from the infection group, which implied the infection relevance of ACs and BAs to SaB. In contrast, LPCs did not show remarkable SaB infection relevance or mortality relevance, probably owing to the general consistency of this class of compounds for SaB disease. We performed pathway enrichment analysis for these three classes of significant compounds (HS versus HM group, Q-value < 0.05). The results of BAs showed that four compounds exhibited metabolic pathways associated with 'Bile secretion', 'Cholesterol metabolism', and 'Primary bile acid biosynthesis' etc (Fig. S5b). Among them, *beta*GCS was a class of compounds with the same parent nucleus. The results for LPCs suggested that compounds with similar parent nucleus structure of LPCs implied association with a series of downstream pathways (Fig. S5c). The significant compounds of ACs were not enriched in the pathway. But, A fundamental role of ACs in tuning the switch between the glucose and fatty acid metabolism was reviewed[53]. Their function implemented via bi-directional transport of acyl moieties Between cytosol and mitochondria (Fig. S5a).

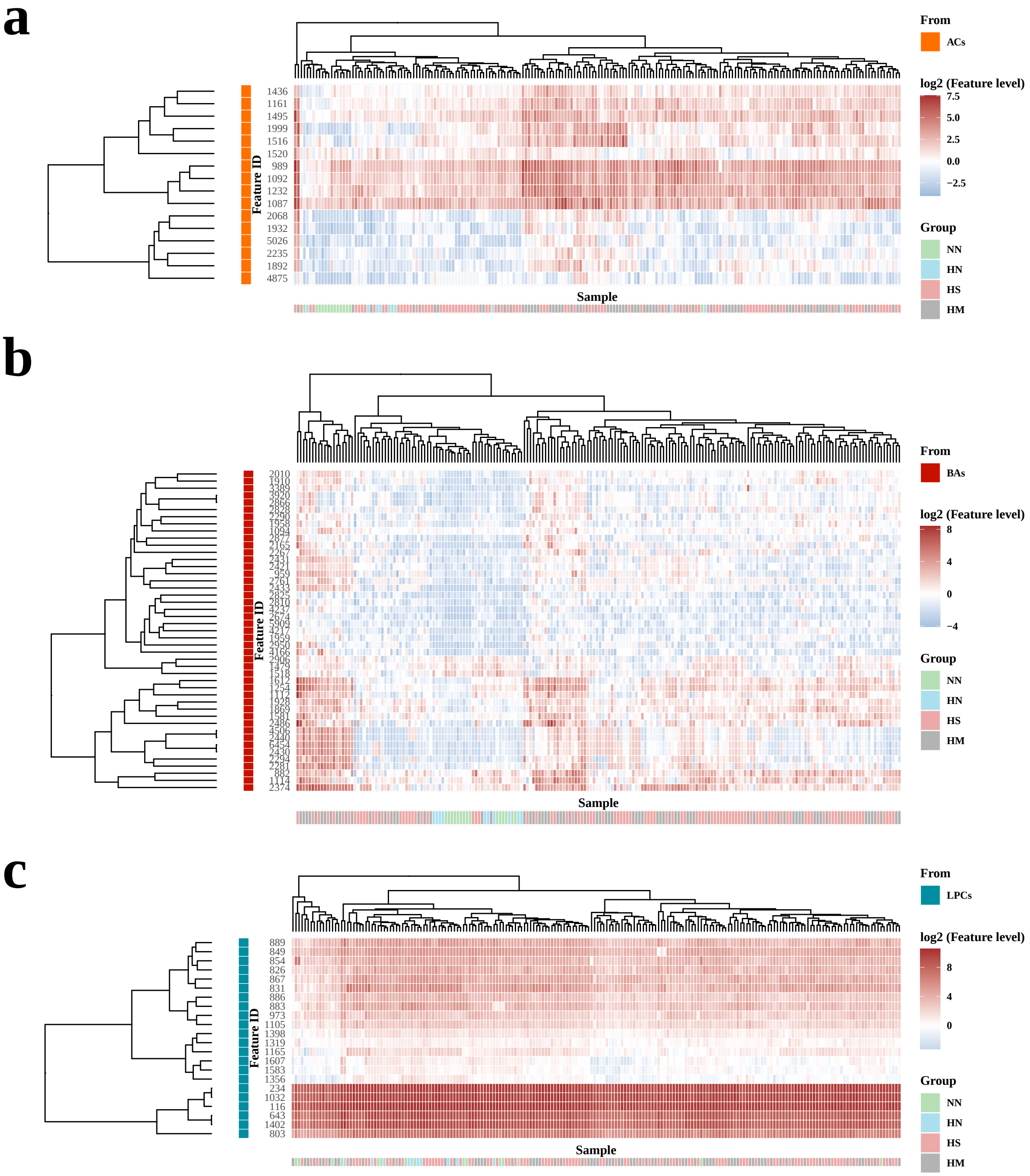

Figure 6: **Heat maps of 'Acyl carnitines' (ACs), 'Lysophosphatidylcholines' (LPCs), 'Bile acids, alcohols and derivatives' (BAs) in serum metabolomics dataset.** Figure 6**a**, **c** and **e** show heat maps of level of ACs, LPCs and BAs. The 'features' are select by either in infection groups versus control groups or HM versus HS group: Q-value < 0.05, $|\log_2(\text{FC})| \geq 0.3$.

In research of Wozniak et al[42], five ACs compounds were identified. In addition, four top metabolites (2-Hexadecanoylthio-1-Ethylphosphorylcholine (HEPC); sphingosine-1-phosphate (S1P); decanoyl-carnitine; L-Thyroxine (T4)) were also identified. In our reanalysis, all identifications were in line except for HEPC (see 'Data and code availability' section for the report of serum dataset analysis). In our re-analysis, ‘HEPC’ was identified as 1-pentadecanoyl-sn-glycero-3-phosphocholine (LPC15:0) or its stereoisomers. Indeed, HEPC and LPC15:0 are quite similar in structure, but distinct in element constitution (corresponding to $C_{23}H_{48}NO_5PS$ and $C_{23}H_{48}NO_7P$ respectively). They were clearly distinct in terms of chemical classification. HEPC belongs to ‘Cholines’ (level 5) from ‘Organic nitrogen compounds’ (superclass) family, whereas LPC15:0 belongs to ‘Lysophosphatidylcholines’ (level 5) from ‘Lipids and lipid-like molecules’ family. As a part of MCnebula workflow, sulfur element is detectable for SIRIUS in isotopes pattern with high mass accuracy[37]. However, for the MS/MS spectra of ‘HEPC’, there was no candidate formula that containing sulfur element. Overall, we identified more compounds with the MCnebula workflow and many of the results were in line with the analysis of Wozniak et al[42]. All identified compounds were collated in Tab. S2 (filtered with Tanimoto similarity > 0.5 and de-duplicated with the first hash block of InChIKey (molecular skeleton)). The compounds (top 50 of EFS and MWU) that were not successfully identified via spectral library matching by Wozniak et al. but were identified by our MCnebula workflow for molecular formula or chemical structure were additionally collated (Tab. S3).

Herbal medicine analysis. We used MCnebula to interpretate structure diversity and chemical transformation during traditional processing of a representative herbal medicine, *Eucommiae Cortex,* the peel of *Eucommia ulmoides Oliv. (E. ulmoides)*[54]. After being processed with saline water, it is commonly applied to treat renal diseases for a long time in China but the chemical basis still remained to be explored. With the help of ABC selection algorithm in MCnebula, a total of 29 chemical classes representing the richness of composition of E. ulmoides were obtained. Two groups of quantification data were performed with binary comparison. The top 20 features (Top20) were selected using function ‘select_features’ ($|\text{Log2(Fold change)}| > 0.3$, Q-value < 0.05, Tanimoto similarity > 0.5) and were traced in Child-Nebulae (Fig. S6). We used MCnebula to draw the mirrored match of MS/MS spectra and extracted ions chromatography (EIC) plots of the Top20 (Fig. S7 and S8). According to Fig. S8, we speculated that the ‘features’ of ID 1642, 1785, and 2321 were newly generated compounds because the peak area levels before the processing were almost zero compared to those after processing. Their chemical structures are showed in Fig. S7. Among them, the ‘feature’ of ID 1642 has a higher probability of correct identification (Tanimoto similarity: 0.69). Based on Fig. S6, we knew that ‘feature’ of ID 1642 belongs to ‘Iridoids and derivatives’ (IAD), the others were ‘Dialkyl ethers’ (DE; ID 1785) and ‘Phenylpropanoids and polyketides’ (PAP; ID 2321). We annotated in depth of the Child-Nebulae of IAD, DE and PAP respectively. The locations of the ‘features’ of ID 1642, 1785 and 2321 in the Child-Nebulae were interrogated (Fig. S9a, b, and c). Only the ‘features’ of ID 1642 had neighboring ‘features’ and their identified chemical structures (ID 2110 and ID 854) had similar parent nuclei. The ‘features’ of ID 2110 and ID 854 were identified with chemical structure (Tanimoto similarity: 0.69 and 0.7 respectively) (Fig. S9d, e, and f); their levels of peak area were decreased and increased after the processing. Based on the chemical structures shown in Fig. S9d and e, we speculated that the compound of ID 2110 was partially converted to the compound of ID 854 after the processing, which may involve chemical changes such as dehydration and rearrangement. Such speculation explained the alteration of the levels of peak area. In addition, the increasement in the level of the compound ID 1642 (its spectra were shown in Fig. S7 and S8) may also be associated with the reduction of the compound ID 2110.

The methods of MCnebula we have demonstrated for discovering significant compounds and discovering chemical changes can be applied to explore more compounds in Tab. S4, but we would not expand on this description here.

Discussion

The analysis of LC-MS/MS data is challenging because of its large dataset and the potential information of the unknown compounds as well as the limited of reference spectral library. Researchers often need to take much time on mapping the landscape of all the interesting compounds from this “black box”, and then move to next step in research MCnebula could assist researchers in focusing on potential markers or interesting compounds quickly by combining full-spectrum identification with machine prediction, visualization of subnebulae in a multi-dimensional view, and statistical analysis to track top ‘features’ and find analogues. The ABC selection algorithm can summarize a representative chemical class in a dataset and obtain the features to that class, so the overall direction of the study is unbiased. Also, it is an effective guarantee for statistical analysis to produce top features for tracing analysis in next step. The results of statistical analysis based on feature level may cause bias since the loss of information, filtering on the basis of chemical classes level can prevent the bias in some degree. The Child-Nebula, which mapped on the basis of the chemical classes obtained by the ABC selection algorithm, achieved the goal of visualizing the huge untargeted dataset as a single graph. Above all, the parameters of the ABC selection algorithm were subjectively adjustable and they should be determined according to the richness of the chemical class of the studied object. In general, our default parameters used to acquire the chemical classes that are abundant in variety according to the datasets and filtered out those that were too large or too small classes in conceptual scope.

For identification, spectral library matching is still the main method for LC-MS/MS data because of its high accuracy. The general classifying of compounds is also based on it, i.e., the chemical structure is firstly identified by spectral matching, and then its chemical class is evaluated based on the chemical structure. Considering the limit of reference spectral library, The classifying technique like CANOPUS[34]incorporated in MCnebula bypassed the first step of identifying the chemical structure but predicted the possible chemical class even if the exact chemical structure was not known. MCnebula combined this cutting-edge technology with ABC selection algorithm and achieve visualization of Child-Nebulae, which make it possible to explore unknown compounds that beyond spectral library. We compared the classifying method of MCnebula with GNPS, of which method relies on chemical structure identification. When different levels of noise were added, the number of classified compounds of GNPS decreased remarkably compared with the stable performance of MCnebula. For the actual acquired MS/MS spectra, they were not as good as the reference spectra and contained some noise. Indeed ,the reality of MS/MS spectra is much closer to the condition with noise. It means MCnebula can resist noise interference in some extent. At the end of the evaluation, we examined the accuracy of the identification by MCnebula. It confirmed that the accuracy of identification fluctuated around 70%, which was the same as SIRIUS[22].

Serum metabolomics data was applied to illustrate that MCnebula can be used for pathway analysis and biomarker discovery. Most of our results were consistent with that of reference[42]. The exciting thing was that that we identified more metabolites that beyond the scope of spectral library matching. Three of the four top metabolites identified by Wozniak et al. were the same as our re-identification, but only one metabolite was controversial. Wozniak et al. mentioned ACs compounds had correlation with SaB disease and ACs compounds were also re-identified in our study. Wozniak et al. used a joint approach of Ensemble Feature Selection (EFS) and Mann-Whitney U (MWU) tests to screen top metabolites[42]. When we compared the 50 top 'features' obtained by the 'binary comparison' method integrated in MCnebula with the top 50 metabolites (top 50 of EFS and 50 of MWU) obtained by the joint method of W et al., a total of 37 overlapped metabolites were screened out, including the key metabolite of L-Thyroxine in the reference study. Top 'features' were usually different according to the feature selection algorithm. The reliability of the 'binary comparison' method was verified again by our ranked results comparing with those of Wozniak et al. In addition to the consistent parts, , more interesting results about other chemical classes associated with SaB disease were revealed by MCnebula. We discovered additional classes, i.e. 'Lysophosphatidylcholines' (LPCs) and 'Bile acids, alcohols and derivatives' (BAs), that were not concerned in previous study. Acutally, LPCs have been extensively investigated in the context of inflammation and atherosclerosis development[52,55,56]. In a recent review[55], the complex roles of LPCs in vascular inflammation were well described, involving the context-dependent pro- or anti-inflammatory action, impact in innate immune cells and adaptive immune system, etc. Decreasing level of LPCs was associated with wild range of diseases of increasing mortality risk[52]. The investigation of spesis indicated LPCs concentrations in blood were established correlation with severe sepsis or septic shock[56]. LPCs was reported inversely correlated with mortality in sepsis patients[57]. BAs' disorder implied a liver dysfunction and imbalance of intestinal microphylactic homeostasis[58]. The chemical multiversity of BAs, which were discovered in the BAs' child-nebula, were determined by the intestinal microbiome and allowed for a complex regulation of adaptive responses in host. In our study, the level of BAs showed higher correlation with SaB infection than ACs. The decreased level of LPCs suggested a mortality risk of SaB infection. From LPCs to BAs, steroids related classes, 'Lineolic acids and derivatives', and other fatty acids related classes, showed that liver played a central role in SaB infection and mortality. Liver X receptors (LXRs) played pivotal roles in the transcriptional control of lipid metabolism[59]. LXRs modulated membrane phospholipid composition through activation of lysophosphatidylcholine acyltransferase 3 (LPCAT3), which was directly related to LPCs[60]. The above classes showed correlation with LXRs[59]. Unfortunately, LXRs' specific role in SaB infection or mortality has not been reported and beyond the scope of this research.

In herbal dataset analysis, MCnebula provided a quick annotation of compounds and exploration of chemical changes in Child-Nebulae with a scope of chemical classes. The main components of *E. ulmoides* were lignans, iridoids, phenolics, flavonoids, steroid and terpenoids[61]. In our study, the chemical classes that obtained by ABC selection algorithm included 'Lignans, neolignans and related compounds' (LNARC) and 'Iridoids and derivatives' (IAD), as well as 'Monoterpenoids' and 'Terpene glycosides'. The flavonoids were covered by 'Phenylpropanoids and polyketides' (PAP)[24] and phenolics may be found in 'Methoxyphenols'. The flavonoids were similar to the steroids and were not retained in selected results as 'Flavonoides' and 'Steroids and steroid derivatives', because they were not as abundant in *E. ulmoides* (bark) as LNARC and IAD. Many of the compounds that identified in chemical classes of LNARC and IAD (Tab. S1) were reported in previous research about LC-MS/MS analysis of *E. ulmoides*[62,63]. We obtained top features based on statistical comparison of the changes in 'features' quantification levels before and after processing. One of the compounds that changed significantly or even was newly produced (ID: 1642) was traced in the Child-Nebulae. We hypothesized that it was related to two structurally similar compounds by transformation. The application of MCnebula in the analysis of plant-derived compounds was well illustrated with this example, particular for quick identification and exploration of chemical changes. Notably, the reference spectral library or database for plant-derived compounds was much more scarce compared with reference spectral library for human-derived metabolites, Although some specific database of plant-derived compounds was constructed[64], there were lack of enough fragmentation spectra for comprehensive library match. With the help of MCnebula, a rapid and reliable resolution of complex compositions of plant-derived can be achieved.

Conclusion

The analysis of LC-MS/MS data is challenging because of its large dataset and much information of the unknown compounds as well as the limited of reference spectral library. Thus, we established a framework called MCnebula to facilitate mass spectrometry data analysis by focusing on critical chemical classes and visualization in multiple dimensions. MCnebula was proposed and implemented in the R language with package of MCnebula. As an integrated visualization method, MCnebula may be more popular for researchers without background of bioinformatics and computer science. According to the results of method evaluation, MCnebula had a lower relative false rate of classified accuracy and its accuracy of identification was up to 70%. In order to illustrate the broad utility of MCnebula, we investigated a human-derived serum dataset for metabolomics analysis. The results indicated that 'Acyl carnitines' were screened out by tracing structural classes of biomarkers which was consistent with the reference. We also investigated a plant-derived dataset of herbal E. ulmoides to achieve a rapid unknown compound annotation and discovery. MCnebula has a great potential in the field of chemistry and biology. In the future, we hope that fields of application of MCnebula could expand to agriculture, food science, medicine and so on.

Acknowledgements

This work was financially supported by the National Natural Science Foundation of China (No. 81922073), Zhejiang Province Traditional Chinese Medicine Science and Technology Project (Nos. 2022ZQ033).

Reference

(1) Tsugawa, H.; Ikeda, K.; Takahashi, M.; Satoh, A.; Mori, Y.; Uchino, H.; Okahashi, N.; Yamada, Y.; Tada, I.; Bonini, P.; Higashi, Y.; Okazaki, Y.; Zhou, Z.; Zhu, Z.-J.; Koelmel, J.; Cajka, T.; Fiehn, O.; Saito, K.; Arita, M.; Arita, M. A Lipidome Atlas in MS-DIAL 4. *Nature Biotechnology* **2020**, *38* (10), 1159–1163. https://doi.org/10.1038/s41587-020-0531-2.

(2) Chong, J.; Soufan, O.; Li, C.; Caraus, I.; Li, S.; Bourque, G.; Wishart, D. S.; Xia, J. MetaboAnalyst 4.0: Towards More Transparent and Integrative Metabolomics Analysis. *Nucleic Acids Research* **2018**, *46* (W1), W486–W494. https://doi.org/10.1093/nar/gky310.

(3) Tsugawa, H. Computational MS/MS Fragmentation and Structure Elucidation Using MS-FINDER Software. In *Comprehensive Natural Products III*; Elsevier, 2020; pp 189–210. https://doi.org/10.1016/B978-0-12-409547-2.14645-1.

(4) Wang, M.; Carver, J. J.; Phelan, V. V.; Sanchez, L. M.; Garg, N.; Peng, Y.; Nguyen, D. D.; Watrous, J.; Kapono, C. A.; Luzzatto-Knaan, T.; Porto, C.; Bouslimani, A.; Melnik, A. V.; Meehan, M. J.; Liu, W.-T.; Crüsemann, M.; Boudreau, P. D.; Esquenazi, E.; Sandoval-Calderón, M.; Kersten, R. D.; Pace, L. A.; Quinn, R. A.; Duncan, K. R.; Hsu, C.-C.; Floros, D. J.; Gavilan, R. G.; Kleigrewe, K.; Northen, T.; Dutton, R. J.; Parrot, D.; Carlson, E. E.; Aigle, B.; Michelsen, C. F.; Jelsbak, L.; Sohlenkamp, C.; Pevzner, P.; Edlund, A.; McLean, J.; Piel, J.; Murphy, B. T.; Gerwick, L.; Liaw, C.-C.; Yang, Y.-L.; Humpf, H.-U.; Maansson, M.; Keyzers, R. A.; Sims, A. C.; Johnson, A. R.; Sidebottom, A. M.; Sedio, B. E.; Klitgaard, A.; Larson, C. B.; Boya P, C. A.; Torres-Mendoza, D.; Gonzalez, D. J.; Silva, D. B.; Marques, L. M.; Demarque, D. P.; Pociute, E.; O'Neill, E. C.; Briand, E.; Helfrich, E. J. N.; Granatosky, E. A.; Glukhov, E.; Ryffel, F.; Houson, H.; Mohimani, H.; Kharbush, J. J.; Zeng, Y.; Vorholt, J. A.; Kurita, K. L.; Charusanti, P.; McPhail, K. L.; Nielsen, K. F.; Vuong, L.; Elfeki, M.; Traxler, M. F.; Engene, N.; Koyama, N.; Vining, O. B.; Baric, R.; Silva, R. R.; Mascuch, S. J.; Tomasi, S.; Jenkins, S.; Macherla, V.; Hoffman, T.; Agarwal, V.; Williams, P. G.; Dai, J.; Neupane, R.; Gurr, J.; Rodríguez, A. M. C.; Lamsa, A.; Zhang, C.; Dorrestein, K.; Duggan, B. M.; Almaliti, J.; Allard, P.-M.; Phapale, P.; Nothias, L.-F.; Alexandrov, T.; Litaudon, M.; Wolfender, J.-L.; Kyle, J. E.; Metz, T. O.; Peryea, T.; Nguyen, D.-T.; VanLeer, D.; Shinn, P.; Jadhav, A.; Müller, R.; Waters, K. M.; Shi, W.; Liu, X.; Zhang, L.; Knight, R.; Jensen, P. R.; Palsson, B. Ø.; Pogliano, K.; Linington, R. G.; Gutiérrez, M.; Lopes, N. P.; Gerwick, W. H.; Moore, B. S.; Dorrestein, P. C.; Bandeira, N. Sharing and Community Curation of Mass Spectrometry Data with Global Natural Products Social Molecular Networking. *Nature Biotechnology* **2016**, *34* (8), 828–837. https://doi.org/10.1038/nbt.3597.

(5) Chambers, M. C.; Maclean, B.; Burke, R.; Amodei, D.; Ruderman, D. L.; Neumann, S.; Gatto, L.; Fischer, B.; Pratt, B.; Egertson, J.; Hoff, K.; Kessner, D.; Tasman, N.; Shulman, N.; Frewen, B.; Baker, T. A.; Brusniak, M.-Y.; Paulse, C.; Creasy, D.; Flashner, L.; Kani, K.; Moulding, C.; Seymour, S. L.; Nuwaysir, L. M.; Lefebvre, B.; Kuhlmann, F.; Roark, J.; Rainer, P.; Detlev, S.; Hemenway, T.; Huhmer, A.; Langridge, J.; Connolly, B.; Chadick, T.; Holly, K.; Eckels, J.; Deutsch, E. W.; Moritz, R. L.; Katz, J. E.; Agus, D. B.; MacCoss, M.; Tabb, D. L.; Mallick, P. A Cross-Platform Toolkit for Mass Spectrometry and Proteomics. *Nature Biotechnology* **2012**, *30* (10), 918–920. https://doi.org/ghh626.

(6) Röst, H. L.; Sachsenberg, T.; Aiche, S.; Bielow, C.; Weisser, H.; Aicheler, F.; Andreotti, S.; Ehrlich, H.-C.; Gutenbrunner, P.; Kenar, E.; Liang, X.; Nahnsen, S.; Nilse, L.; Pfeuffer, J.; Rosenberger, G.; Rurik, M.; Schmitt, U.; Veit, J.; Walzer, M.; Wojnar, D.; Wolski, W. E.; Schilling, O.; Choudhary, J. S.; Malmström, L.; Aebersold, R.; Reinert, K.; Kohlbacher, O. OpenMS: A Flexible Open-Source Software Platform for Mass Spectrometry Data Analysis. *Nature Methods* **2016**, *13* (9), 741–748. https://doi.org/f82r32.

(7) Smith, C. A.; Want, E. J.; O'Maille, G.; Abagyan, R.; Siuzdak, G. XCMS: Processing Mass Spectrometry Data for Metabolite Profiling Using Nonlinear Peak Alignment, Matching, and Identification. *Analytical Chemistry* **2006**, *78* (3), 779–787. https://doi.org/b58xrd.

(8) Pluskal, T.; Castillo, S.; Villar-Briones, A.; Orešič, M. MZmine 2: Modular Framework for Processing, Visualizing, and Analyzing Mass Spectrometry-Based Molecular Profile Data. *BMC Bioinformatics* **2010**, *11* (1), 395. https://doi.org/bxbwnj.

(9) Myers, O. D.; Sumner, S. J.; Li, S.; Barnes, S.; Du, X. One Step Forward for Reducing False Positive and False Negative Compound Identifications from Mass Spectrometry Metabolomics Data: New Algorithms for Constructing Extracted Ion Chromatograms and Detecting Chromatographic Peaks. *Analytical Chemistry* **2017**, *89* (17), 8696–8703. https://doi.org/gbrjtm.

(10) Fu, J.; Zhang, Y.; Wang, Y.; Zhang, H.; Liu, J.; Tang, J.; Yang, Q.; Sun, H.; Qiu, W.; Ma, Y.; Li, Z.; Zheng, M.; Zhu, F. Optimization of Metabolomic Data Processing Using NOREVA. *Nature Protocols* **2022**, *17* (1), 129–151. https://doi.org/10.1038/s41596-021-00636-9.

(11) Mahieu, N. G.; Patti, G. J. Systems-Level Annotation of a Metabolomics Data Set Reduces 25 000 Features to Fewer Than 1000 Unique Metabolites. *Analytical Chemistry* **2017**, *89* (19), 10397–10406. https://doi.org/10.1021/acs.analchem.7b02380.

(12) Gloaguen, Y.; Kirwan, J. A.; Beule, D. Deep Learning-Assisted Peak Curation for Large-Scale LC-MS Metabolomics. *Analytical Chemistry* **2022**, *94* (12), 4930–4937. https://doi.org/10.1021/acs.analchem.1c02220.

(13) Wang, M.; Jarmusch, A. K.; Vargas, F.; Aksenov, A. A.; Gauglitz, J. M.; Weldon, K.; Petras, D.; da Silva, R.; Quinn, R.; Melnik, A. V.; van der Hooft, J. J. J.; Caraballo-Rodríguez, A. M.; Nothias, L. F.; Aceves, C. M.; Panitchpakdi, M.; Brown, E.; Di Ottavio, F.; Sikora, N.; Elijah, E. O.; Labarta-Bajo, L.; Gentry, E. C.; Shalapour, S.; Kyle, K. E.; Puckett, S. P.; Watrous, J. D.; Carpenter, C. S.; Bouslimani, A.; Ernst, M.; Swafford, A. D.; Zúñiga, E. I.; Balunas, M. J.; Klassen, J. L.; Loomba, R.; Knight, R.; Bandeira, N.; Dorrestein, P. C. Mass Spectrometry Searches Using MASST. *Nature Biotechnology* **2020**, *38* (1), 23–26. https://doi.org/10.1038/s41587-019-0375-9.

(14) Wolf, S.; Schmidt, S.; Müller-Hannemann, M.; Neumann, S. In Silico Fragmentation for Computer Assisted Identification of Metabolite Mass Spectra. *BMC Bioinformatics* **2010**, *11* (1), 148. https://doi.org/10.1186/1471-2105-11-148.

(15) Allen, F.; Greiner, R.; Wishart, D. Competitive Fragmentation Modeling of ESI-MS/MS Spectra for Putative Metabolite Identification. *Metabolomics* **2015**, *11* (1), 98–110. https://doi.org/10.1007/s11306-014-0676-4.

(16) Ruttkies, C.; Schymanski, E. L.; Wolf, S.; Hollender, J.; Neumann, S. MetFrag Relaunched: Incorporating Strategies Beyond in Silico Fragmentation. *Journal of Cheminformatics* **2016**, *8*, 3. https://doi.org/10.1186/s13321-016-0115-9.

(17) Blaženović, I.; Kind, T.; Torbašinović, H.; Obrenović, S.; Mehta, S. S.; Tsugawa, H.; Wermuth, T.; Schauer, N.; Jahn, M.; Biedendieck, R.; Jahn, D.; Fiehn, O. Comprehensive Comparison of in Silico MS/MS Fragmentation Tools of the CASMI Contest: Database Boosting Is Needed to Achieve 93% Accuracy. *Journal of Cheminformatics* **2017**, *9* (1), 32. https://doi.org/10.1186/s13321-017-0219-x.

(18) Kind, T.; Liu, K.-H.; Lee, D. Y.; DeFelice, B.; Meissen, J. K.; Fiehn, O. LipidBlast in Silico Tandem Mass Spectrometry Database for Lipid Identification. *Nature Methods* **2013**, *10* (8), 755–758. https://doi.org/10.1038/nmeth.2551.

(19) Heinonen, M.; Shen, H.; Zamboni, N.; Rousu, J. Metabolite Identification and Molecular Fingerprint Prediction Through Machine Learning. *Bioinformatics (Oxford, England)* **2012**, *28* (18), 2333–2341. https://doi.org/10.1093/bioinformatics/bts437.

(20) Dührkop, K.; Shen, H.; Meusel, M.; Rousu, J.; Böcker, S. Searching Molecular Structure Databases with Tandem Mass Spectra Using CSI:FingerID. *Proceedings of the National Academy of Sciences* **2015**, *112* (41), 12580–12585. https://doi.org/10.1073/pnas.1509788112.

(21) Ludwig, M.; Dührkop, K.; Böcker, S. Bayesian Networks for Mass Spectrometric Metabolite Identification via Molecular Fingerprints. *Bioinformatics (Oxford, England)* **2018**, *34* (13), i333–i340. https://doi.org/10.1093/bioinformatics/bty245.

(22) Dührkop, K.; Fleischauer, M.; Ludwig, M.; Aksenov, A. A.; Melnik, A. V.; Meusel, M.; Dorrestein, P. C.; Rousu, J.; Böcker, S. SIRIUS 4: A Rapid Tool for Turning Tandem Mass Spectra into Metabolite Structure Information. *Nature Methods* **2019**, *16* (4), 299–302. https://doi.org/10.1038/s41592-019-0344-8.

(23) Ashburner, M.; Ball, C. A.; Blake, J. A.; Botstein, D.; Butler, H.; Cherry, J. M.; Davis, A. P.; Dolinski, K.; Dwight, S. S.; Eppig, J. T.; Harris, M. A.; Hill, D. P.; Issel-Tarver, L.; Kasarskis, A.; Lewis, S.; Matese, J. C.; Richardson, J. E.; Ringwald, M.; Rubin, G. M.; Sherlock, G. Gene Ontology: Tool for the Unification of Biology. The Gene Ontology Consortium. *Nature Genetics* **2000**, *25* (1), 25–29. https://doi.org/10.1038/75556.

(24) Djoumbou Feunang, Y.; Eisner, R.; Knox, C.; Chepelev, L.; Hastings, J.; Owen, G.; Fahy, E.; Steinbeck, C.; Subramanian, S.; Bolton, E.; Greiner, R.; Wishart, D. S. ClassyFire: Automated Chemical Classification with a Comprehensive, Computable Taxonomy. *Journal of Cheminformatics* **2016**, *8* (1), 61. https://doi.org/10.1186/s13321-016-0174-y.

(25) Blaženović, I.; Kind, T.; Sa, M. R.; Ji, J.; Vaniya, A.; Wancewicz, B.; Roberts, B. S.; Torbašinović, H.; Lee, T.; Mehta, S. S.; Showalter, M. R.; Song, H.; Kwok, J.; Jahn, D.; Kim, J.; Fiehn, O. Structure Annotation of All Mass Spectra in Untargeted Metabolomics. *Analytical chemistry* **2019**, *91* (3), 2155–2162. https://doi.org/10.1021/acs.analchem.8b04698.

(26) Ernst, M.; Kang, K. B.; Caraballo-Rodríguez, A. M.; Nothias, L.-F.; Wandy, J.; Chen, C.; Wang, M.; Rogers, S.; Medema, M. H.; Dorrestein, P. C.; van der Hooft, J. J. J. MolNetEnhancer: Enhanced Molecular Networks by Integrating Metabolome Mining and Annotation Tools. *Metabolites* **2019**, *9* (7). https://doi.org/10.3390/metabo9070144.

(27) Lee, J.; da Silva, R. R.; Jang, H. S.; Kim, H. W.; Kwon, Y. S.; Kim, J.-H.; Yang, H. In Silico Annotation of Discriminative Markers of Three Zanthoxylum Species Using Molecular Network Derived Annotation Propagation. *Food chemistry* **2019**, *295*, 368–376. https://doi.org/10.1016/j.foodchem.2019.05.099.

(28) Sha, B.; Schymanski, E. L.; Ruttkies, C.; Cousins, I. T.; Wang, Z. Exploring Open Cheminformatics Approaches for Categorizing Per- and Polyfluoroalkyl Substances (PFASs). *Environmental science. Processes & impacts* **2019**, *21* (11), 1835–1851. https://doi.org/10.1039/c9em00321e.

(29) Tripathi, A.; Vázquez-Baeza, Y.; Gauglitz, J. M.; Wang, M.; Dührkop, K.; Nothias-Esposito, M.; Acharya, D. D.; Ernst, M.; van der Hooft, J. J. J.; Zhu, Q.; McDonald, D.; Brejnrod, A. D.; Gonzalez, A.; Handelsman, J.; Fleischauer, M.; Ludwig, M.; Böcker, S.; Nothias, L.-F.; Knight, R.; Dorrestein, P. C. Chemically Informed Analyses of Metabolomics Mass Spectrometry Data with Qemistree. *Nature Chemical Biology* **2021**, *17* (2), 146–151. https://doi.org/10.1038/s41589-020-00677-3.

(30) Wishart, D. S. Emerging Applications of Metabolomics in Drug Discovery and Precision Medicine. *Nature Reviews. Drug Discovery* **2016**, *15* (7), 473–484. https://doi.org/10.1038/nrd.2016.32.

(31) Guma, M.; Tiziani, S.; Firestein, G. S. Metabolomics in Rheumatic Diseases: Desperately Seeking Biomarkers. *Nature Reviews. Rheumatology* **2016**, *12* (5), 269–281. https://doi.org/10.1038/nrrheum.2016.1.

(32) Degenhardt, F.; Seifert, S.; Szymczak, S. Evaluation of Variable Selection Methods for Random Forests and Omics Data Sets. *Briefings in Bioinformatics* **2019**, *20* (2), 492–503. https://doi.org/10.1093/bib/bbx124.

(33) Neumann, U.; Genze, N.; Heider, D. EFS: An Ensemble Feature Selection Tool Implemented as R-package and Web-Application. *BioData Mining* **2017**, *10* (1), 21. https://doi.org/10.1186/s13040-017-0142-8.

(34) Dührkop, K.; Nothias, L.-F.; Fleischauer, M.; Reher, R.; Ludwig, M.; Hoffmann, M. A.; Petras, D.; Gerwick, W. H.; Rousu, J.; Dorrestein, P. C.; Böcker, S. Systematic Classification of Unknown Metabolites Using High-Resolution Fragmentation Mass Spectra. *Nature Biotechnology* **2021**, *39* (4), 462–471. https://doi.org/10.1038/s41587-020-0740-8.

(35) Platten, M.; Nollen, E. A. A.; Röhrig, U. F.; Fallarino, F.; Opitz, C. A. Tryptophan Metabolism as a Common Therapeutic Target in Cancer, Neurodegeneration and Beyond. *Nature Reviews Drug Discovery* **2019**, *18* (5), 379–401. https://doi.org/gfvk74.

(36) Watrous, J.; Roach, P.; Alexandrov, T.; Heath, B. S.; Yang, J. Y.; Kersten, R. D.; van der Voort, M.; Pogliano, K.; Gross, H.; Raaijmakers, J. M.; Moore, B. S.; Laskin, J.; Bandeira, N.; Dorrestein, P. C. Mass Spectral Molecular Networking of Living Microbial Colonies. *Proceedings of the National Academy of Sciences* **2012**, *109* (26), E1743–E1752. https://doi.org/10.1073/pnas.1203689109.

(37) Böcker, S.; Letzel, M. C.; Lipták, Z.; Pervukhin, A. SIRIUS: Decomposing Isotope Patterns for Metabolite Identification†. *Bioinformatics* **2009**, *25* (2), 218–224. https://doi.org/10.1093/bioinformatics/btn603.

(38) Dührkop, K.; Böcker, S. Fragmentation Trees Reloaded. In *Research in Computational Molecular Biology*; Przytycka, T. M., Ed.; Springer International Publishing: Cham, 2015; Vol. 9029, pp 65–79. https://doi.org/10.1007/978-3-319-16706-0_10.

(39) Ludwig, M.; Nothias, L.-F.; Dührkop, K.; Koester, I.; Fleischauer, M.; Hoffmann, M. A.; Petras, D.; Vargas, F.; Morsy, M.; Aluwihare, L.; Dorrestein, P. C.; Böcker, S. Database-Independent Molecular Formula Annotation Using Gibbs Sampling Through ZODIAC. *Nature Machine Intelligence* **2020**, *2* (10), 629–641. https://doi.org/10.1038/s42256-020-00234-6.

(40) Smyth, G. K. Limma: Linear Models for Microarray Data. In *Bioinformatics and Computational Biology Solutions Using R and Bioconductor*; Gentleman, R., Carey, V. J., Huber, W., Irizarry, R. A., Dudoit, S., Eds.; Springer-Verlag: New York, 2005; pp 397–420. https://doi.org/10.1007/0-387-29362-0_23.

(41) Law, C. W.; Zeglinski, K.; Dong, X.; Alhamdoosh, M.; Smyth, G. K.; Ritchie, M. E. A Guide to Creating Design Matrices for Gene Expression Experiments. *F1000Research* **2020**, *9*, 1444. https://doi.org/10.12688/f1000research.27893.1.

(42) Wozniak, J. M.; Mills, R. H.; Olson, J.; Caldera, J. R.; Sepich-Poore, G. D.; Carrillo-Terrazas, M.; Tsai, C.-M.; Vargas, F.; Knight, R.; Dorrestein, P. C.; Liu, G. Y.; Nizet, V.; Sakoulas, G.; Rose, W.; Gonzalez, D. J. Mortality Risk Profiling of Staphylococcus Aureus Bacteremia by Multi-omic Serum Analysis Reveals Early Predictive and Pathogenic Signatures. *Cell* **2020**, *182* (5), 1311–1327.e14. https://doi.org/10.1016/j.cell.2020.07.040.

(43) Xie, Y.; Dervieux, C.; Riederer, E. *R Markdown Cookbook*; Chapman and Hall/CRC: Boca Raton, Florida, 2020.

(44) Hoffmann, M. A.; Nothias, L.-F.; Ludwig, M.; Fleischauer, M.; Gentry, E. C.; Witting, M.; Dorrestein, P. C.; Dührkop, K.; Böcker, S. High-Confidence Structural Annotation of Metabolites Absent from Spectral Libraries. *Nature Biotechnology* **2021**. https://doi.org/10.1038/s41587-021-01045-9.

(45) Guha, R. Chemical Informatics Functionality in R. *Journal of Statistical Software* **2007**, *18* (6).

(46) Temple Lang, D. *RCurl: General Network (HTTP/FTP/...) Client Interface for R*; 2022.

(47) Pletnev, I.; Erin, A.; McNaught, A.; Blinov, K.; Tchekhovskoi, D.; Heller, S. InChIKey Collision Resistance: An Experimental Testing. *Journal of Cheminformatics* **2012**, *4* (1), 39. https://doi.org/10.1186/1758-2946-4-39.

(48) Pang, Z.; Chong, J.; Li, S.; Xia, J. MetaboAnalystR 3.0: Toward an Optimized Workflow for Global Metabolomics. *Metabolites* **2020**. https://doi.org/10.3390/metabo10050186.

(49) Picart-Armada, S.; Fernandez-Albert, F.; Vinaixa, M.; Yanes, O.; Perera-Lluna, A. FELLA: An R Package to Enrich Metabolomics Data. *BMC Bioinformatics* **2018**, *19* (1), 538. https://doi.org/10.1186/s12859-018-2487-5.

(50) Lai, J.; Huang, L.; Bao, Y.; Wang, L.; Lyu, Q.; Kuang, H.; Wang, K.; Sang, X.; Yang, Q.; Shan, Q.; Cao, G. A Deep Clustering-Based Mass Spectral Data Visualization Strategy for Anti-Renal Fibrotic Lead Compound Identification from Natural Products. *The Analyst* **2022**, *147* (21), 4739–4751. https://doi.org/10.1039/D2AN01185A.

(51) Chen, Y.-H.; Bi, J.-H.; Xie, M.; Zhang, H.; Shi, Z.-Q.; Guo, H.; Yin, H.-B.; Zhang, J.-N.; Xin, G.-Z.; Song, H.-P. Classification-Based Strategies to Simplify Complex Traditional Chinese Medicine (TCM) Researches Through Liquid Chromatography-Mass Spectrometry in the Last Decade (2011–2020): Theory, Technical Route and Difficulty. *Journal of Chromatography A* **2021**, *1651*, 462307. https://doi.org/10.1016/j.chroma.2021.462307.

(52) Krautbauer, S.; Eisinger, K.; Wiest, R.; Liebisch, G.; Buechler, C. Systemic Saturated Lysophosphatidylcholine Is Associated with Hepatic Function in Patients with Liver Cirrhosis. *Prostaglandins & Other Lipid Mediators* **2016**, *124*, 27–33. https://doi.org/10.1016/j.prostaglandins.2016.06.001.

(53) Melone, M. A. B.; Valentino, A.; Margarucci, S.; Galderisi, U.; Giordano, A.; Peluso, G. The Carnitine System and Cancer Metabolic Plasticity. *Cell Death & Disease* **2018**, *9* (2), 228. https://doi.org/10.1038/s41419-018-0313-7.

(54) Huang, L.; Lyu, Q.; Zheng, W.; Yang, Q.; Cao, G. Traditional Application and Modern Pharmacological Research of Eucommia Ulmoides Oliv. *Chinese Medicine* **2021**, *16* (1), 73. https://doi.org/gnmwxx.

(55) Knuplez, E.; Marsche, G. An Updated Review of Pro- and Anti-Inflammatory Properties of Plasma Lysophosphatidylcholines in the Vascular System. *International Journal of Molecular Sciences* **2020**, *21* (12), E4501. https://doi.org/10.3390/ijms21124501.

(56) Park, D. W.; Kwak, D. S.; Park, Y. Y.; Chang, Y.; Huh, J. W.; Lim, C.-M.; Koh, Y.; Song, D.-K.; Hong, S.-B. Impact of Serial Measurements of Lysophosphatidylcholine on 28-Day Mortality Prediction in Patients Admitted to the Intensive Care Unit with Severe Sepsis or Septic Shock. *Journal of Critical Care* **2014**, *29* (5), 882.e5–11. https://doi.org/10.1016/j.jcrc.2014.05.003.

(57) Drobnik, W.; Liebisch, G.; Audebert, F.-X.; Fröhlich, D.; Glück, T.; Vogel, P.; Rothe, G.; Schmitz, G. Plasma Ceramide and Lysophosphatidylcholine Inversely Correlate with Mortality in Sepsis Patients. *Journal of Lipid Research* **2003**, *44* (4), 754–761. https://doi.org/10.1194/jlr.M200401-JLR200.

(58) Perino, A.; Demagny, H.; Velazquez-Villegas, L.; Schoonjans, K. Molecular Physiology of Bile Acid Signaling in Health, Disease, and Aging. *Physiological Reviews* **2021**, *101* (2), 683–731. https://doi.org/10.1152/physrev.00049.2019.

(59) Wang, B.; Tontonoz, P. Liver X Receptors in Lipid Signalling and Membrane Homeostasis. *Nature Reviews. Endocrinology* **2018**, *14* (8), 452–463. https://doi.org/10.1038/s41574-018-0037-x.

(60) Zhang, Q.; Yao, D.; Rao, B.; Jian, L.; Chen, Y.; Hu, K.; Xia, Y.; Li, S.; Shen, Y.; Qin, A.; Zhao, J.; Zhou, L.; Lei, M.; Jiang, X.-C.; Cao, Y. The Structural Basis for the Phospholipid Remodeling by Lysophosphatidylcholine Acyltransferase 3. *Nature Communications* **2021**, *12* (1), 6869. https://doi.org/10.1038/s41467-021-27244-1.

(61) Huang, L.; Lyu, Q.; Zheng, W.; Yang, Q.; Cao, G. Traditional Application and Modern Pharmacological Research of Eucommia Ulmoides Oliv. *Chinese medicine* **2021**, *16* (1), 73. https://doi.org/10.1186/s13020-021-00482-7.

(62) Huang, Y.-X.; Liu, E.-W.; Wang, L.; Huo, Y.; Wang, Q.; Olaleye, O.; Wang, T.; Gao, X.-M. LC/MS/MS Determination and Pharmacokinetic Studies of Six Compounds in Rat Plasma Following Oral Administration of the Single and Combined Extracts of Eucommia Ulmoides and Dipsacus Asperoides. *Chinese journal of natural medicines* **2014**, *12* (6), 469–476. https://doi.org/10.1016/S1875-5364(14)60073-X.

(63) Hu, F.; An, J.; Li, W.; Zhang, Z.; Chen, W.; Wang, C.; Wang, Z. UPLC-MS/MS Determination and Gender-Related Pharmacokinetic Study of Five Active Ingredients in Rat Plasma After Oral Administration of Eucommia Cortex Extract. *Journal of ethnopharmacology* **2015**, *169*, 145–155. https://doi.org/10.1016/j.jep.2015.04.007.

(64) Sawada, Y.; Nakabayashi, R.; Yamada, Y.; Suzuki, M.; Sato, M.; Sakata, A.; Akiyama, K.; Sakurai, T.; Matsuda, F.; Aoki, T.; Hirai, M. Y.; Saito, K. RIKEN Tandem Mass Spectral Database (ReSpect) for Phytochemicals: A Plant-Specific MS/MS-based Data Resource and Database. *Phytochemistry* **2012**, *82*, 38–45. https://doi.org/10.1016/j.phytochem.2012.07.007.